arXiv:hep-ph/0410385v1 28 Oct 2004

SUSY: THEORY STATUS IN THE LIGHT OF EXPERIMENTAL CONSTRAINTS

Alexander Belyaev

Department of Physics, Florida State University
Tallahassee, FL 32306, USA
E-mail: belyaev@hep.fsu.edu

Abstract. Supersymmetry remains compelling theory over 30 years in spite of lack of its discovery. It could be already near the corner our days, therefore present and upcoming experiments are crucial for constraining or even discovery of the supersymmetry.

INTRODUCTION

Since 1970's the Standard Model (SM) based on local gauge invariance principle explains all experimental data with a good precision. It is based on $SU(3)_c \times SU(2)_L \times U(1)_Y$ non-Abelian Yang-Mills type gauge theory spontaneously broken to $SU(3)_c \times U(1)_Y$ group.

Interestingly, at about the same time, when SM has been established, the first ideas of Supersymmetry appeared independently around the world: "Extension of the algebra of Poincaré group generators and violation of P invariance" of Golfand and Likhtman (1971) [1], "Dual theory for free fermions" of Ramon (1971) [2], "Quark model of dual pions" of Neveu and Schwarz (1971) [3], "Is the neutrino a Goldstone particle?" of Volkov and Akulov (1973) [4]. One should mention separately the work of Wess and Zumino, "Supergauge transformations in four-dimensions" (1974) [5], where the first 4D supersymmetric quantum field theory has been formulated, which has caused the great escalation of the interest of physics community in supersymmetric theories.

Supersymmetry is the symmetry, which relates bosons and fermions and transforms them one into another by acting with supersymmetric fermionic generators Q:

$$Q|\text{BOSON}\rangle = |\text{FERMION}\rangle, \quad Q|\text{FERMION}\rangle = |\text{BOSON}\rangle \tag{1}$$

One can consider Supersymmetry as one of the most promising attempts to understand and explain the origin of the fundamental difference between the two classes of particles – bosons and fermions. This is already itself quite a reason for the theoretical attractiveness of the Supersymmetry. Supersymmetry predicts "mirror" particles to those of the SM, which we know. These supersymmetric partners should differ from their SM partners by spin $1/2$ and have the same mass if the Supersymmetry is unbroken. Since it is not the case, and we do not observe this "mirror" supersymmetric world, one can conclude that Supersymmetry either does not take place or it is broken. This review is

about the second option, since – as author will try to convince you – there is a big chance that Supersymmetry did realized in nature.

Supersymmetry was invented more then 30 years ago but still had not been found yet. However, people are publishing thousands of papers on Supersymmetry per year till present time and the annual number of the papers does not go down as one can see from Fig. 1. What makes SUSY being so attractive in spite of the 30 years unsuccessful hunting for it?! There are several fundamental reasons for this.

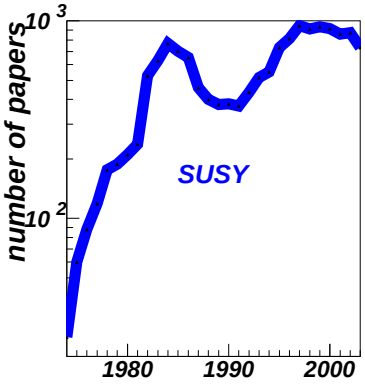


FIGURE 1. The number of papers published on Supersymmetry versus time

One of them is that super-Poincaré group – the group of the Supersymmetry – contains the most fundamental set of space-time symmetries as was shown by Haag, Lopusanski and Sohnius in 1975 [6]. It contains space-time symmetries of the Poincaré group and includes in addition the supersymmetry transformation, linking therefore bosons and fermions. It would be strange if the nature did not use this complete set of symmetries.

Besides this, the requirement for supersymmetric transformation to be *local* yields spin-2 massless gauge filed, the graviton, mediating gravitational interactions [7, 8, 9]. Therefore, Supersymmetry could provide unification of all forces in Nature, including gravity.

Supersymmetry also allows to include fermions into Supestring theories which solve the problem of non-renormalizability of the gravitational theory and pretend to solve the ultimate goal of construction of theory of everything.

Eventually, the ideas of Supersymmetry – yet a pure theoretical invention – survived for more than 30 years because our common belief in unification.

Miraculous consequence of the Supersymmetry is the prediction of the *unification of the gauge couplings* and solution of the *gauge hierarchy problem* which are central theoretical problems of the SM. In SM one can calculate the evolution of the gauge coupling with the energy scale by running respective β-functions. Evolution of $SU(3)$, $SU(2)$ and $U(1)$ coupling from electroweak (EW) scale up to the $10^{15} - 10^{16}$GeV (GUT) scale does not give point-like unification of electromagnetic, electroweak and strong forces in case of the SM (Fig. 2, left frame). In case of minimal Supersymmetric extension of the SM (MSSM), SUSY particles modify beta-functions at about 1 TeV scale and all three couplings do meet together around $M_{GUT} \sim 10^{16}$ GeV (Fig. 2, right).

It is worth to stress that attractive features of the supersymmetry mentioned above, which solve principal theoretical problems of the SM are only *consequences* (which has been derived many years after the SUSY has been formulated!) of the supersymmetry. This fact makes SUSY really attractive from the theoretical point of view.

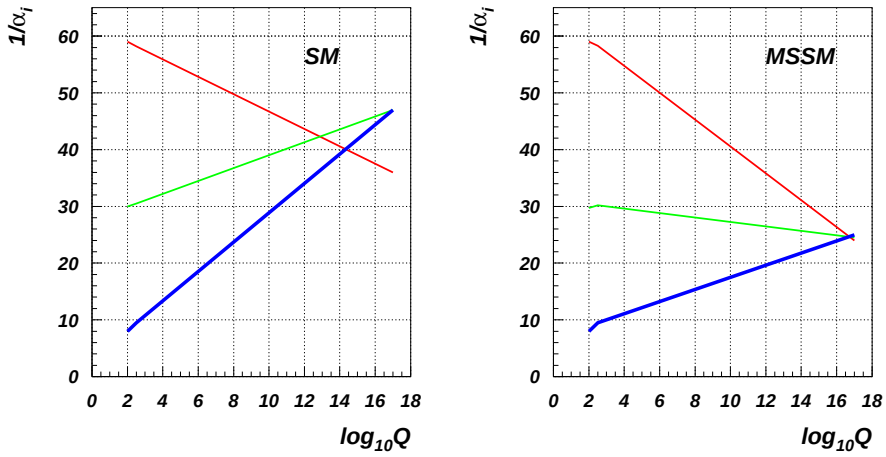


FIGURE 2. Evolution of the inverse coupling in the SM (left) and MSSM (right).

SUPERSYMMETRIC GENERALIZATION OF THE STANDARD MODEL

This overview is aimed at giving the current status of SUSY in the light of present phenomenological and experimental constraints. Therefore the detailed review of basics of Supersymmetry (see *e.g.* [10, 11, 12, 13, 14, 15]) is outside of the scope of this paper and will be very brief here.

Supersymmetry relates bosons and fermions, which transform one into another under the action of fermionic generators of supersymmetry algebra Q and $\overline{Q}$. Therefore the Poincaré algebra has to include commutators of 4-momentum and angular momentum operators P_μ and $M_{\mu\nu}$ with the new fermionic generators Q_α and $\overline{Q}_{\dot{\alpha}}$ as well as the anticommutator of Q_α and $\overline{Q}_{\dot{\alpha}}$:

$$\left[P^\mu, Q_\alpha\right] = 0, \quad \left[M^{\mu\nu}, Q_\alpha\right] = -i(\sigma^{\mu\nu})^\beta_\alpha Q_\beta, \quad \left\{Q_\alpha, Q_\beta\right\} = 0, \quad \left\{\overline{Q}_\alpha, \overline{Q}_{\dot{\beta}}\right\} = 0, \quad \left\{Q_\alpha, \overline{Q}_{\dot{\beta}}\right\} = 2\sigma^\mu_{\alpha\dot{\beta}} P_\mu \tag{2}$$

One can see from (2) that consequent application of two supersymmetry transformations leads to the usual space-time translation generated by P^μ, which tells us that Supersymmetry is a space-time symmetry. Furthermore, making SUSY local, one obtains General Relativity, or theory of gravity, or supergravity [7, 8, 9].

In the simplest case, there is one pair of Q and $\overline{Q}$ ($N = 1$ supersymmetry in contrast with extended supersymmetries with $N \geq 2$). $N = 1$ is the case of our focus here in constructing a supersymmetric version of the Standard Model.

Superfield formalism is the most convenient way for constructing supersymmetric lagrangians. Ordinary fields in this formalism are being extended to *superfields* which are functions of space-time coordinates and anti-commuting Grassmann coordinates θ^α and $\overline{\theta}^{\dot{\beta}}$ ($\alpha, \dot{\beta} = 1, 2$). There are two kinds of superfields participating in construction of SUSY lagrangian: *chiral superfield*, Φ and *vector superfield*, V. Chiral superfield contains chiral supermultiplet: $\Phi \sim (A, \psi, F)$, where $A(x)$ is the complex scalar field, $\psi(x)$

is the complex Weyl spinor and $F(x)$ is the auxiliary scalar field, which is being eliminated by equations of motions and which is needed to close the supersymmetric algebra. Vector superfield contains $V \sim (\lambda, v_\mu, D)$, where λ is a Weyl fermion, v_μ is the vector (gauge) field and D is the auxiliary field. When constructing SUSY Lagrangian it is convenient to define *field strength tensor* (an analog of $F_{\mu\nu}$ in the non-supersymmetric field theory):
$W_\alpha = -\frac{1}{4}\overline{D}^2 e^V D_\alpha e^{-V}$, and $\overline{W}_{\dot\alpha} = -\frac{1}{4} D^2 e^V \overline{D}_{\dot\alpha} e^{-V}$
where D and $\bar{D}$ are covariant derivatives: $D^\alpha = -\partial^\alpha + i(\bar\theta\bar\sigma)^{\mu\alpha}\partial_\mu$, $\bar{D}^{\dot\alpha} = \bar\partial^{\dot\alpha} - i(\bar\sigma\theta)^{\mu\dot\alpha}\partial_\mu$,
and $\sigma^\mu = (1, \sigma^i)$, $\bar\sigma^\mu = (1, -\sigma^i)$, are Pauli matrices ($i = 1-3$).

The MSSM Lagrangian should consists of two parts — SUSY generalization of the Standard Model and SUSY-breaking part (since we do not observe exact SUSY): $\mathscr{L}_{MSSM} = \mathscr{L}_{SUSY} + \mathscr{L}_{breaking}$, with $\mathscr{L}_{SUSY} = \mathscr{L}_{Gauge} + \mathscr{L}_{Gauge-matter} + \mathscr{L}_{matter} =$

$$\sum_{Gauge} \frac{1}{4}\left(\int d^2\theta\ TrW^\alpha W_\alpha + h.c.\right) + \sum_{Matter} \int d^2\theta d^2\bar\theta\ \Phi_i^\dagger e^{\sum_{Gauge} g_j \hat{V}_j} \Phi_i + \int d^2\theta \mathscr{W} \quad (3)$$

where $\mathscr{W}$ is a superpotential, which should be invariant under the group of symmetry of a particular model and has the following general form:

$$\int d^2\theta\ [\lambda_i \Phi_i + \frac{1}{2} m_{ij}\Phi_i\Phi_j + \frac{1}{3} y_{ijk}\Phi_i\Phi_j\Phi_k] + h.c. \quad (4)$$

The general form of written above superpotential does not forbid violation of baryon (B) and lepton (L) numbers. The simultaneous presence of both B- and L- violating interactions should be forbidden since it leads to the fast proton decay. To avoid this problem one can impose a new discrete symmetry, called R-parity: $R = (-1)^{3(B-L)+2S}$, where S is the spin of the particle. All ordinary Standard Model particles have $R = 1$, the superpartners have $R = -1$. R-parity implies that the superparticles can be produced only in pairs and that the lightest supersymmetric particle (LSP) is *stable*, which is a very welcome crucial point making LSP the best cold dark matter candidate. In the MSSM one assumes that R-parity is conserved.

When constructing MSSM – minimal supersymmetric extension of the Standard Model – one should note that numbers of degrees of freedom of bosons and fermions should be the same, *and* bosonic and fermionic superpartners should have the same quantum numbers. Looking at the quantum numbers of the SM particles one concludes that *new fermions* – gauginos (gluino, wino, zino, photino and two higgsinos) – should be added to be the superpartners of *known bosons* and *new bosons (scalars)* – squarks and sleptons – should be added to be the superpartners of *known fermions*.

The important feature of the supersymmetric models is the enlarged Higgs sector. In particular, Higgs sector of the MSSM has the additional Higgs doublet. One of the reasons for it is that in supersymmetric model higgsino has the contribution to the gauge anomaly, therefore one needs two higgsinos with opposite hypercharges to realize the cancellation of the gauge anomaly. Hence one needs *two* Higgs doublets with opposite hypercharges to make such a cancellation possible. Another reason for the introduction

	Superfield	Bosons	Fermions	$SU_C(3), SU_L(2), U_Y(1)$
Gauge	$\mathbf{G^a}$	gluon g^a	gluino $\tilde{g}^a$	(8,1,0)
	$\mathbf{V^k}$	Weak W^k $(W^{\pm}, Z)$	wino, zino $\tilde{w}^k$ $(\tilde{w}^{\pm}, \tilde{z})$	(1,3,0)
	$\mathbf{V'}$	Hypercharge B (γ)	bino $\tilde{b}(\tilde{\gamma})$	(1,1,0)
Matter	$\mathbf{L_i}$	sleptons $\tilde{L}_i = (\tilde{\nu}, \tilde{e})_L$	leptons $L_i = (\nu, e)_L$	$(1,2,-1)$
	$\mathbf{E_i}$			$(1,1,2)$
	$\mathbf{Q_i}$	squarks $\tilde{Q}_i = (\tilde{u}, \tilde{d})_L$	quarks $Q_i = (u,d)_L$	$(3,2,1/3)$
	$\mathbf{U_i}$			$(\bar{3},1,-4/3)$
	$\mathbf{D_i}$			$(3,1,2/3)$
Higgs	$\mathbf{H_1}$	Higgses H_1 $(h, H, A, H^{\pm})$	higgsinos $\tilde{H}_1$ $(\tilde{h_1}, \tilde{h_2}, \tilde{h}^{\pm})$	$(1,2,-1)$
	$\mathbf{H_2}$			$(1,2,1)$

TABLE 1. MSSM particle contents and respective $SU(3) \times SU(2) \times U(1)$ quantum numbers

of additional Higgs doublet is to give masses for both up- and down- type quarks. Conjugated Higgs field cannot be used in MSSM (like it was done in SM) since $\Phi\Phi\Phi^{\dagger}$ form (which would appear in this analogy) is not chiral superfield and therefore is not supersymmetric.

Table 1 summarizes the particle contents and the quantum numbers of the MSSM.

The SUSY breaking sector is one of the most essential in MSSM model. We do not observe degenerate states of particles and anti-particles, which unavoidably leads to conclusion that SUSY should be broken. The implementation of SUSY breaking should not spoil the cancellation of the quadratic divergences i.e. SUSY should be broken *softly*. The most general form of the soft SUSY part should include operators with mass dimension ≤ 4 [16]:

$$-\mathscr{L}_{soft} = \sum_{scalars} m_{ij} A_i^* A_j + \sum_{gauginos} M_a \left(\lambda_a \lambda_a + \bar{\lambda}_a \bar{\lambda}_a\right) + \sum_{i,j,k} A_{ijk} \lambda_{ijk} A_i A_j A_k + \mu B H_1 H_2 \tag{5}$$

This general form $\mathscr{L}_{soft}$, which includes many parameters, should be properly constrained in order to address the experimental non-observation of flavor and CP-violating processes.

It is known that none of the fields of the MSSM can develop nonzero vacuum expectation value (v.e.v.) to break SUSY without spoiling gauge invariance. In the most common scenarios SUSY breaking occur in the *hidden sector* and propagates to the *visible sector* via *messengers*. There are several known mechanisms to mediate SUSY breaking from hidden to visible sector: gravity mediation (SUGRA), gauge mediation (GMSB), anomaly mediation (AMSB) and gaugino mediation (inoMSB).

In SUGRA scenario [17, 18, 19] the hidden sector communicates with visible one via gravity, leading to the SUSY breaking scale $M_{\not{SUSY}} \sim m_{3/2}$, where $m_{3/2}$ is the gravitino mass. Scalar masses m_{ij}, gaugino masses M_a and trilinear couplings are proportional to $m_{3/2}$ but can be non-universal in general. In this case one should properly address flavor and CP problem. In minimal SUGRA scenario the universality hypothesis of equal boundary conditions at the GUT scale greatly reduces the number of parameters down to four: m_0 – the common scalar mass, $m_{1/2}$ – the common gaugino mass, A_0 and B –

the common tri- and bilinear soft supersymmetry breaking parameters at the GUT scale and allows to solve the flavor and CP problem.

In the case of gauge mediation, messenger is not gravity but superfield Φ that couples to hidden sector and SM fields via gauge interactions [20, 21, 22]. In this scenario gaugino masses are generated at 1-loop level: $M_a = \frac{g_a^2}{16\pi^2}\frac{\langle F_S\rangle}{M}$ (M is the messenger mass scale, while $\langle F_S\rangle$ is the v.e.v. of singlet scalar superfield of the hidden sector), while sfermion masses are generated at 2-loop level: $\tilde{m}_A^2 = 2\sum C_a^A \left(\frac{g_a^2}{16\pi^2}\right)^2 \left(\frac{\langle F_S\rangle}{M}\right)^2$. Remarkable feature of this scenario is that Gravitino is LSP since $m_{\tilde{G}} \sim \frac{\langle F_S\rangle}{M}\cdot\frac{M}{M_{PL}}$ is suppressed by Plank Mass. Another specific feature of this scenario is that soft masses are correlated to the respective gauge couplings.

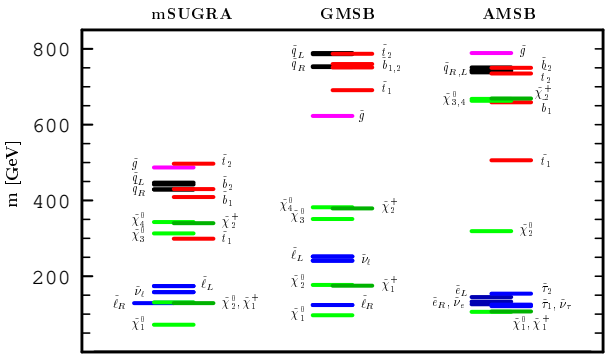


FIGURE 3. Sample spectra for SUSY particles for SUGRA, GMSB and AMSB scenarios [23]

Anomaly mediation as well as Gaugino mediation scenarios are based on the paradigm of extra-dimensional brane world. Anomaly mediated SUSY breaking [24, 25] is generated due to conformal (super-Weyl) anomaly at 1-loop level while SUGRA mediation effects are exponentially suppressed since hidden and visible sectors reside on different branes. In gaugino mediated scenario [26, 27], again, hidden and visible sectors are on different branes while gravity and gauge fields are propagate in the bulk and directly couple fields on both branes. As a result, gauginos acquire mass but scalar masses are suppressed and may be neglected at the GUT scale.

The mechanism of SUSY breaking determines the sparticle spectrum and therefore is crucial for the SUSY phenomenology and particle searches. Fig. 3 from [23] presents the sample spectra for three of four models mentioned above.

HUNTING FOR SUPERSYMMETRY

General strategy

The search for the weak scale Supersymmetry is one of the prime objectives of present and future experiments.

As we discussed above, supersymmetric models can be classified by the mechanism for communicating SUSY breaking from the hidden sector to the observable sector. Among those scenarios SUGRA could be considered as the most conservative, since it requires neither extra dimensions nor new messenger fields while gravity does exist.

The so-called *minimal* supergravity (mSUGRA) model has traditionally been the most popular choice for phenomenological SUSY analyses. In mSUGRA, it is assumed that the MSSM is valid from the weak scale all the way up to the GUT scale $M_{GUT} \simeq 10^{16}$ GeV, where the gauge couplings unify. For this model a simple choice of Kähler metric

and gauge kinetic function led to *universal* soft SUSY breaking scalar masses (m_0), gaugino masses ($m_{1/2}$) and A-terms (A_0) at M_{GUT}. This assumption of universality leads to the phenomenologically motivated suppression of flavor changing neutral current (FCNC) processes. However, there is no known physical principle which gives rise to the desired form of Kähler metric and gauge kinetic function, and in general non-universal soft breaking mass parameters at the GUT scale are expected [28, 29]. In addition, quantum corrections would lead to large deviations from universality at the tree-level [30].

We will also require that electroweak symmetry is broken radiatively (REWSB), allowing us to fix the magnitude (not the sign) of the superpotential Higgs mass term μ to obtain the correct value of M_Z. The bilinear soft supersymmetry breaking (SSB) parameter B is usually traded for $\tan\beta$ (the ratio of Higgs field vacuum expectation values). Thus, the parameter set

$$m_0,\ m_{1/2},\ A_0,\ \tan\beta,\ \text{ and }\ sign(\mu) \tag{6}$$

completely determines the spectrum of supersymmetric matter and Higgs fields. The results presented in this review are based on ISASUGRA program, the part of the ISAJET [31] package, which calculates the SUSY particle mass spectrum. ISASUGRA includes full one-loop radiative corrections to all sparticle masses and Yukawa couplings, and minimizes the scalar potential using the renormalization group improved 1-loop effective potential including all tadpole contributions, evaluated at an optimized scale choice which accounts for leading two loop terms. Working in the $\overline{DR}$ regularization scheme, the weak scale values of gauge and third generation Yukawa couplings are evolved via 2-loop RGEs to M_{GUT}. At M_{GUT}, universal SSB boundary conditions are imposed, and all SSB masses along with gauge and Yukawa couplings are evolved to the weak scale M_{weak}. Using an optimized scale choice $Q_{SUSY} = \sqrt{m_{\tilde{t}_L} m_{\tilde{t}_R}}$, the RG-improved one-loop effective potential is minimized and the entire spectrum of SUSY and Higgs particles is calculated. There is generally a good agreement between Isajet spectrum and publicly available SoftSUSY [32], Spheno [33] and Suspect [34] codes, as detailed in Ref. [35].

Once the SUSY and Higgs masses and mixings are known, then one should calculate observables and compare them against experimental constraints. The most important of these are: cold dark matter (CDM) bounds as well as direct and indirect CDM search experiments; bounds from various collider experiments (including the future ones) – LEP, TEVATRON, LHC, NLC; rare decay processes such as $b \to s\gamma$, $B_S \to \mu^+\mu^-$, $\mu \to e\gamma$; electric and dipole moments e.g. δa_μ – anomalous magnetic muon moment; measurement of the proton life time related to SUSY GUTs theories.

Cold dark matter bounds.

Among the most important experiments for SUSY search are those, which confirmed the evidence of cold dark matter (CDM) in the Universe and aimed for direct/indirect search of CDM candidate. The most direct evidence for CDM in the Universe comes from observations of galactic rotation curves. Also binding of galaxies in clusters, matching observations of large scale structure with simulations, gravitational microlensing, baryonic density of the Universe as determined by Big Bang nucleosynthesis, observations of supernovae in distant galaxies, and measurements of anisotropies in the cosmic mi-

crowave background radiation (CMB) can be considered as a confident confirmation of CDM (for reviews see e.g. [36, 37]). In particular, the Wilkinson Microwave Anisotropy Probe (WMAP) [38, 39] collaboration has extracted a variety of cosmological parameters from fits to precision measurements of the CMB radiation. It was found that

$$\Omega_{total} = 1.02 \pm 0.02 \tag{7}$$

where $\Omega_{total} = \rho_{total}/\rho_c$, ρ_{total} is the matter-energy density of the Universe, ρ_c (G_N is the Newton constant) the critical density of the closure of the Universe, defined within Friedman-Robert-Walker (FRW) framework. H is the Hubble parameter usually defined through the rescaled Hubble parameter h as $H = 100h$ Km/(s Mpc). So, with a good precision, Universe has been measured to be flat. The properties of the Universe are characterized by the density of baryons (Ω_b), matter density (Ω_m), vacuum energy (Ω_Λ) and the expansion rate (h) which are measured to be:

$$\Omega_b = 0.044 \pm 0.004, \quad \Omega_m = 0.27 \pm 0.04, \quad \Omega_\Lambda = 0.73 \pm 0.04, \quad h = 0.71^{+0.04}_{-0.03}. \tag{8}$$

From the WMAP results, one derives the following value for CDM:

$$\Omega_{CDM} h^2 = \Omega_m h^2 - \Omega_b h^2 = 0.1126^{+0.0081}_{-0.0090}(^{+0.0161}_{-0.0181}) \text{ at } 68(95)\% \text{ CL}. \tag{9}$$

The energy content of the Universe according to WMAP data is schematically presented in Fig. 4. There exists a number of hypothetical candidate elementary particles to fill the role of CDM. A particularly attractive candidate for CDM is the lightest neutralino in R-parity conserving supersymmetric models [40, 41].

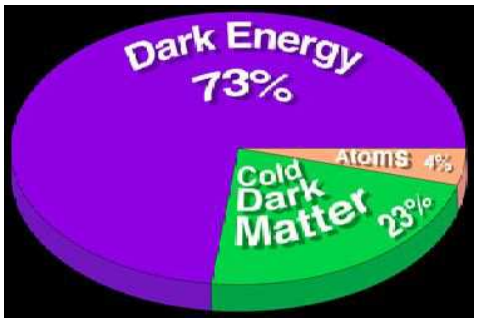


FIGURE 4. The energy content of the Universe according to WMAP data (source: http://map.gsfc.nasa.gov/)

The evolution of the number density of supersymmetric relics in the universe is described by the Boltzmann equation as formulated for a FRW Universe. For calculations including many particle species, such as the case where co-annihilations are important, there is a Boltzmann equation for each particle species [42], the equations can be combined to obtain

$$\frac{dn}{dt} = -3Hn - \langle \sigma_{eff} v \rangle \left(n^2 - n_{eq}^2 \right), \tag{10}$$

where $n = \sum_{i=1}^{N} n_i$, $n_{eq,i} = \frac{g_i m_i^2 T}{2\pi^2} K_2\left(\frac{m_i}{T}\right)$ and the sum extends over the N particle species contributing to the relic density, with n_i being the number density of the i-th species, K_j is a modified Bessel function of the second kind of order j. The quantity $\langle \sigma_{eff} v \rangle$ is the thermally averaged cross section times velocity which is the key point in calculating relic density including co-annihilation processes with $\Omega h^2 \propto 1/[\int_0^{x_F} \langle \sigma_{eff} v \rangle dx]$, where one integrates $\langle \sigma_{eff} v \rangle$ from 0 to freeze-out temperature, x_F [43, 42, 44]. The main challenge in CDM calculation is the evaluation of *all possible channels* for neutralino annihilation to SM and/or Higgs particles, as well as all co-annihilation reactions with *relativistic thermal averaging*. For our calculation of the neutralino relic density, we use

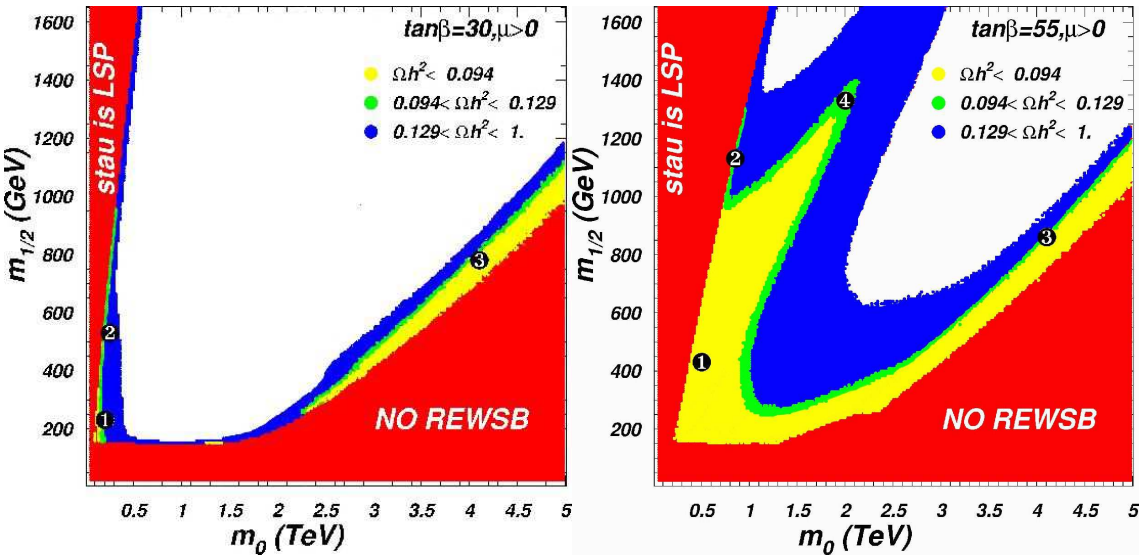


FIGURE 5. Regions of neutralino relic density in the m_0 vs $m_{1/2}$ plane for $A_0 = 0$ and $\tan\beta = 30(55)$. Generic regions which are in agreement with WMAP results: 1) bulk annihilation region, 2) stau co-annihilation region, 3) hyperbolic branch/focus point (HB/FP) region and 4) A-annihilation funnel region (only right plot for high $\tan\beta$).

the IsaReD program [45] interfaced with Isajet. There are also public programs for CDM calculations such DarkSUSY [46, 47] and micrOMEGAs [48, 49] (as well as many private ones) which are in a good agreement with IsaReD. In most of the parameter space of the mSUGRA model, it turns out that a value of $\Omega_{\widetilde{Z}_1} h^2$ well beyond the WMAP bound is generated. Only certain regions of the mSUGRA model parameter space give rise to a relatively low value of $\Omega_{\widetilde{Z}_1} h^2$ in accord with WMAP measurements. Fig. 5 presents such generic regions in m_0 versus $m_{1/2}$ plane for $\mu > 0$, $A_0 = 0$ $\tan\beta = 30, 55$ (left, right). The dark (red) shaded regions are excluded by theoretical constraints (lack of REWSB on the right, a charged LSP in the upper left). The blue (dark-gray) shaded region ($0.129 > \Omega_{\widetilde{Z}_1} h^2 > 1$) and, furthermore, unshaded region ($\Omega_{\widetilde{Z}_1} h^2 > 1$) are excluded, since their too high relic density would lead to overclosure of the Universe contradicting with WMAP data. The green (gray) shaded regions are in exact agreement with WMAP constraints (Eq. 9) and could be classified in several classes:

1. The bulk annihilation region at low values of m_0 and $m_{1/2}$, where neutralino pair annihilation occurs at a large rate via t-channel slepton exchange.
2. The stau co-annihilation region at low m_0 where $m_{\widetilde{Z}_1} \simeq m_{\tilde{\tau}_1}$ so that $\widetilde{Z}_1$s may co-annihilate with $\tilde{\tau}_1$s in the early universe [50, 51].
3. The hyperbolic branch/focus point (HB/FP) region [52, 53, 54, 55] at large m_0 near the boundary of the REWSB excluded region where $|\mu|$ becomes small, and the neutralinos have a significant higgsino component, which facilitates annihilations to WW and ZZ pairs.
4. The A-annihilation funnel, which occurs at very large $\tan\beta \sim 45 - 60$ [56, 57, 58, 59, 60, 61]. In this case, the value of $m_A \sim 2m_{\widetilde{Z}_1}$. An exact equality of the

mass relation isn't necessary, since the A width can be quite large ($\Gamma_A \sim 10-50$ GeV); then $2m_{\widetilde{Z}_1}$ can be several widths away from resonance, and still achieve a large $\widetilde{Z}_1\widetilde{Z}_1 \to A \to f\bar{f}$ annihilation cross section. The heavy scalar Higgs H also contributes to the annihilation cross section.

In addition, there exists a region of neutralino top-squark co-annihilation (for very particular A_0 values) and a light Higgs h annihilation funnel (at low $m_{1/2}$ values). In the light-gray (yellow) region neutralino relic density is too low ($\Omega_{\widetilde{Z}_1}h^2 < 0.096$) to give a good fit for WMAP data. But, strictly speaking, this region is not excluded since there could be *additional* particles (e.g. axions or particles from various models with extra-dimensions) contributing to CDM relic density. Therefore, hereafter we treat green and yellow regions of Fig. 5 as one, allowed ("green") region.

Constraints from LEP2 searches

The LEP2 collaborations have finished taking data and collected the rich statistics for e^+e^- CM energies ranging up to $\sqrt{s} \simeq 208$ GeV. Searches for superpartners at LEP2 gave negative results and led to the following constraints:

$$m_{\widetilde{W}_1} > 103.5\ GeV\ [62], \quad m_{\tilde{e}} > 99\ GeV \ \text{ provided } \ m_{\tilde{\ell}} - m_{\widetilde{Z}_1} < 10\ GeV\ [63] \qquad (11)$$

The LEP2 experiments also searched for the SM Higgs boson. In addition to finding several compelling signal candidates consistent with $m_h \sim 115$ GeV, they set a limit $m_{H_{SM}} > 114.1$ GeV [64]. In our mSUGRA parameter space scans, the lightest SUSY Higgs boson h is almost always SM-like. The exception occurs when the value of m_A becomes low, less than $100-150$ GeV. This Higgs mass LEP2 limit requires radiative corrections to the light Higgs mass (which is below Z-boson mass at the tree level) to be quite large. Those radiative corrections – δM_h – are logarithmically sensitive to the SUSY scale (M_{SUSY}) and this LEP2 limit pushes this to level of $\sim 1\ TeV$. At the same time $\delta M_h \propto m_{top}^4$. In the light of recent m_{top} measurements from D0 [65] which shifted up top-quark mass to be 178.0 ± 4.3 GeV (as a world averaged value) led to some relaxation of the lower limit on M_{SUSY}.

The $b \to s\gamma$ branching fraction

The branching fraction $BF(b \to s\gamma)$ has recently been measured by the BELLE [66], CLEO [67] and ALEPH [68] collaborations. Combining statistical and systematic errors in quadrature, these measurements give $(3.36 \pm 0.67) \times 10^{-4}$ (BELLE), $(3.21 \pm 0.43) \times 10^{-4}$ (CLEO) and $(3.11 \pm 1.07) \times 10^{-4}$ (ALEPH). A weighted averaging of these results yields $BF(b \to s\gamma) = (3.25 \pm 0.37) \times 10^{-4}$. The 95% CL range corresponds to $\pm 2\sigma$ away from the mean. To this we should add uncertainty in the theoretical evaluation, which within the SM dominantly comes from the scale uncertainty, and is about 10%.[1] Together, these imply the bounds,

$$2.2 \times 10^{-4} < BF(b \to s\gamma) < 4.33 \times 10^{-4} \qquad (12)$$

[1] We caution the reader that the SUSY contribution may have a larger theoretical uncertainty, particularly if $\tan\beta$ is large.

Other computations of the range of $BF(b\to s\gamma)$ include for instance Ellis *et al.* [69]: $2.33\times10^{-4} < BF(b\to s\gamma) < 4.15\times10^{-4}$, and Djouadi *et al.* [70]: $2.0\times10^{-4} < BF(b\to s\gamma) < 5.0\times10^{-4}$. In our study, we simply show contours of $BF(b\to s\gamma)$ of 2, 3, 4 and 5×10^{-4}, allowing the reader the flexibility of their own interpretation.

The calculation of $BF(b\to s\gamma)$ used here is based upon the program of Ref. [71, 72]. That calculation uses an effective field theory approach to evaluating radiative corrections to the $b\to s\gamma$ decay rate. In our calculations, we implement the running b-quark mass including SUSY threshold corrections as calculated in ISASUGRA; these effects can be important at large values of the parameter $\tan\beta$ [73, 74]. Once the relevant operators and Wilson coefficients are known at $Q=M_W$, then the SM WCs are evolved down to $Q=m_b$ via NLO RG running. At m_b, the $BF(b\to s\gamma)$ is evaluated at NLO, including bremsstrahlung effects. Our value of the SM $b\to s\gamma$ branching fraction yields 3.4×10^{-4}, with a scale uncertainty of 10%.

Muon anomalous magnetic moment

The muon anomalous magnetic moment $a_\mu = \frac{(g-2)_\mu}{2}$ has been recently measured to high precision by the E821 experiment [75] for the negative muon along with earlier results on the positive muon [76]. In addition, theoretical determinations of $(g-2)_\mu$ have been presented by Davier *et al.* [77] and Hagiwara *et al.* [78] which use recent data on $e^+e^-\to$ *hadrons* at low energy to determine the hadronic vacuum polarization contribution to the muon magnetic moment. Combining the latest experiment and theory numbers, we find the deviation of a_μ to be:

$$\Delta a_\mu = (27.1\pm9.4)\times10^{-10} \quad (\text{Davier } et\ al.) \tag{13}$$

$$\Delta a_\mu = (24.7\pm9.0)\times10^{-10} \quad (\text{Hagiwara } et\ al.). \tag{14}$$

The Davier *et al.* group also presents a number using τ decay data to determine the hadronic vacuum polarization, which gives $\Delta a_\mu = (12.4\pm8.3)\times10^{-10}$, *i.e.* nearly consistent with the SM prediction. However, there seems to be growing consensus that the numbers using the e^+e^- data are to be trusted more, since they offer a direct determination of the hadronic vacuum polarization. The $\sim 3\sigma$ deviation in a_μ using the e^+e^- data can be explained in a supersymmetric context if second generation sleptons (smuons and muon sneutrinos) and charginos and neutralinos are relatively light.

$B_s\to\mu^+\mu^-$ **decay**

While all SUSY models contain two doublets of Higgs superfields, there are no tree-level flavor changing neutral currents because one doublet $\hat{H}_u$ couples only to $T_3=1/2$ fermions, while the other doublet $\hat{H}_d$ couples just to $T_3=-1/2$ fermions. At one loop, however, couplings of $\hat{H}_u$ to down type fermions are induced. These induced couplings grow with $\tan\beta$. As a result, down quark Yukawa interactions and down type quark mass matrices are no longer diagonalized by the same transformation, and flavor violating couplings of neutral Higgs scalars h, H and A emerge. Of course, in the limit of large m_A, the Higgs sector becomes equivalent to the SM Higgs sector with the light Higgs boson $h=H_{SM}$, and the flavor violation decouples. The interesting thing is that while this decoupling occurs as $m_A\to\infty$, *there is no decoupling for sparticle masses becoming large.*

An important consequence of this coupling is the possibility of the decay $B_s \to \mu^+\mu^-$, whose branching fraction has been experimentally bounded by CDF [79] to be:

$$BF(B_s \to \mu^+\mu^-) < 2.6 \times 10^{-6}, \tag{15}$$

mediated by the neutral states in the Higgs sector of supersymmetric models. While this branching fraction is very small within the SM ($BF_{SM}(B_s \to \mu^+\mu^-) \simeq 3.4 \times 10^{-9}$), the amplitude for the Higgs-mediated decay of B_s grows as $\tan^3\beta$ within the SUSY framework, and hence can completely dominate the SM contribution if $\tan\beta$ is large. Several groups [80, 81, 82] and recently [83] have analyzed the implications of this decay within the mSUGRA framework. We also present improved $b \to s\gamma$ branching fraction predictions in accord with [83] for the current ISAJET release. This constraint is important only for very large values of $\tan\beta$.

mSUGRA constraints.

Within the mSUGRA framework, the parameters m_0 and $m_{1/2}$ are the most important for fixing the scale of sparticle masses. The $m_0 - m_{1/2}$ plane (for fixed values of other parameters) is convenient for a simultaneous display of these constraints, and hence, of parameter regions in accord with all experimental data. Physicists interested in the mSUGRA model may wish to focus their attention on these regions.

Our results for combined constraints mentioned above are presented in Fig. 6 for mSUGRA model in the $m0$ vs $m_{1/2}$ plane for $A_0 = 0$ and $\tan\beta$ =30 (55) in the left (right) frame, respectively. Top raw of frames presents constraints themselves, while the bottom raw presents corresponding χ^2 pattern for frames above. χ^2 is formed from Δa_μ, $BF(b \to s\gamma)$ and $\Omega_{\widetilde{Z}_1} h^2$, as given in Eqn's (9,12,14).

Allowed CDM relic density regions are the green shaded ones, LEP2 excluded regions denoted by yellow color. Black contours denotes δa_μ values ($30, 10, 5, 1 \times 10^{-10}$ – from bottom to top) and blue contours denote $BF(b \to s\gamma)$ values ($2, 3 \times 10^{-4}$ – from bottom to top). In the left upper frame of Fig. 6 one can observe the tension between δa_μ and $BF(B \to s\gamma)$. The point is that while $BF(b \to s\gamma)$ favors large third generation squark masses to suppress SUSY contributions to $b \to s\gamma$ decay, Δa_μ experimental value favors relatively light second generation slepton masses, to give a significant $(g-2)_\mu$ deviation from the SM value. This is clearly reflected in the respective (left bottom) frame where the χ^2 quantity is presented.

In case of low and intermediate values of $\tan\beta$ almost all the m_0 *vs.* $m_{1/2}$ plane has very large χ^2. This arises because in general an overabundance of dark matter is produced in the early universe, and the relic density $\Omega_{\widetilde{Z}_1} h^2$ is beyond WMAP limits. There is a very narrow sliver of yellow at $m_{1/2} \sim 150$ GeV (just beyond the LEP2 limit) where $2m_{\widetilde{Z}_1} \simeq m_h$, and neutralinos can annihilate through the narrow light Higgs resonance. In addition, there is an orange/yellow region at high m_0 at the edge of parameter space (the HB/FP region), with an intermediate value of χ^2. In an earlier study [84], this region was found to have a low χ^2 value. In the present situation, however, the 3σ deviation from the SM of a_μ tends to disfavor the HB/FP region. In the HB/FP region, sleptons are so heavy (typically 3-5 TeV), that SUSY contributions to a_μ are tiny, and the prediction is that a_μ should be in near accord with the SM calculation. The remaining green region is the narrow sliver that constitutes the stau co-annihilation

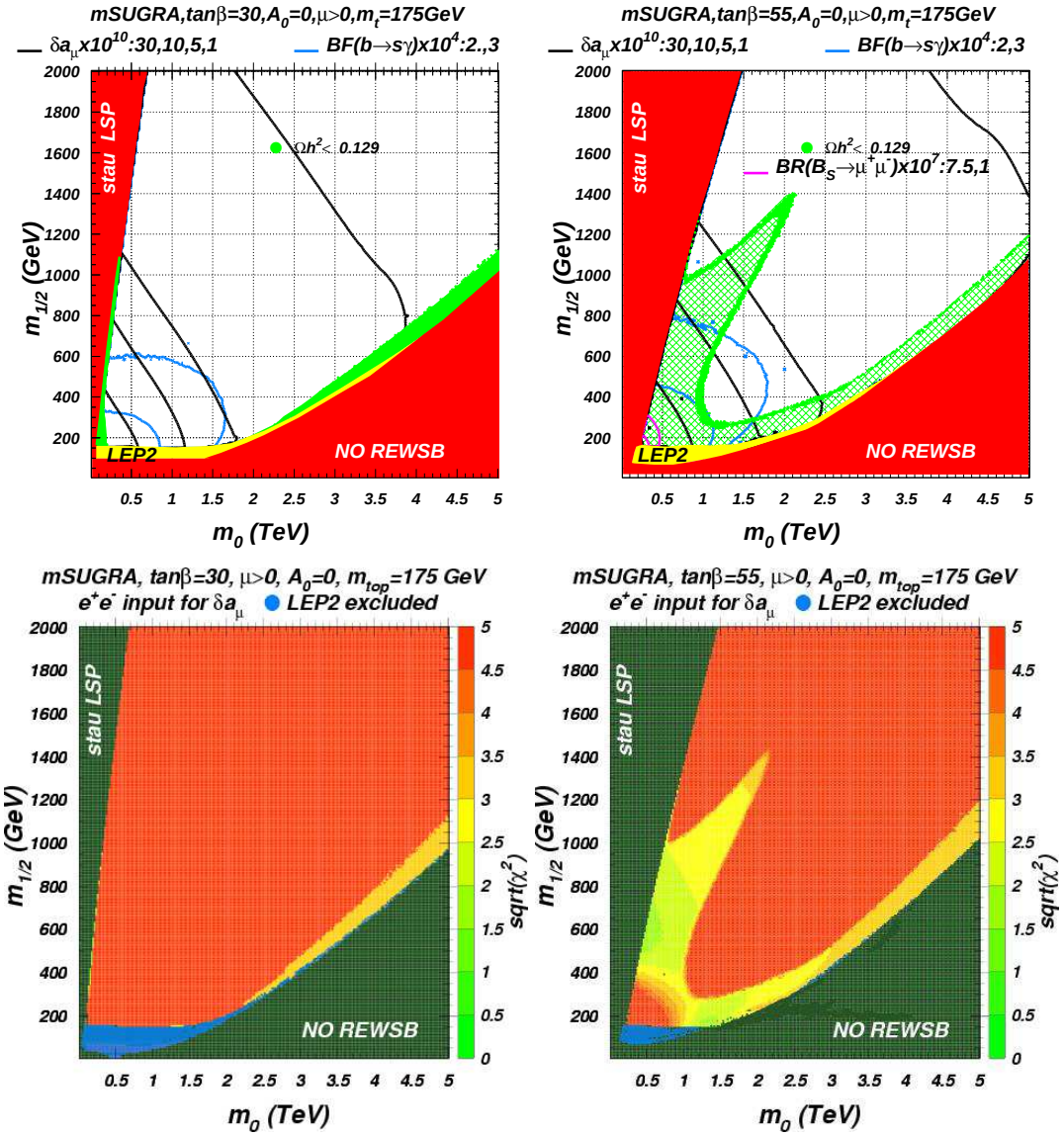


FIGURE 6. Constraints for mSUGRA model in the m_0 vs $m_{1/2}$ plane for $A_0 = 0$ and $\tan\beta = 30(55)$ (top raw). Top raw: allowed CDM relic density regions are the green shaded ones, LEP2 excluded regions denoted by yellow color. Black contours denotes δa_μ values $(30, 10, 5, 1 \times 10^{-10}$ – from bottom to top) and blue contours denote $BF(b \to s\gamma)$ values $(2, 3 \times 10^{-4}$ – from bottom to top). Magenta contours for $BF(B_S \to \mu^+\mu^-)$ are relevant only for very high $\tan\beta = 55$ $(7.5, 1 \times 10^{-7}$ – from bottom to top). The bottom raw of figures presents $\sqrt{\chi^2}$ for the respective parameters of the mSUGRA model. The green regions have low χ^2, while red regions have high χ^2. Yellow is intermediate.

region, barely visible at the left hand edge of parameter space adjacent to where $\tilde{\tau}_1$ becomes the LSP.

Once we move to very large $\tan\beta$ values, as shown in the right set of frames of Fig. 6, then the A-annihilation funnel becomes visible, and some large regions of moderately low χ^2 appear around $m_0,\ m_{1/2} \sim 500,\ 600$ GeV and also at $1500,\ 200$ GeV. While

the A-annihilation funnel extends over a broad region of parameter space, the upper and lower ends of the funnel are disfavored: basically, if sparticles become too heavy (the upper end), then Δa_μ becomes too small, while if sparticles become too light (the lower end), then $BF(b \to s\gamma)$ deviates too much from its central value.

One comes to conclusions [85] that for the mSUGRA model almost all of parameter space is excluded or at least disfavored by the combination of the WMAP $\Omega_{\tilde{Z}_1} h^2$ limit, the new Δa_μ value, and the $BF(b \to s\gamma)$ value. The $\Omega_{\tilde{Z}_1} h^2$ constraint only allows the several regions of parameter space mentioned above, while $BF(b \to s\gamma)$ favors large third generation squark masses to suppress SUSY contributions to $b \to s\gamma$ decay, and Δa_μ favors relatively light second generation slepton masses, to give a significant deviation of $(g-2)_\mu$ from the SM value. The only surviving regions with relatively low $\sqrt{\chi^2} \lesssim 2$ are the stau co-annihilation region, and intermediate portions of the A-annihilation funnel at very large values of $\tan\beta$. One should note, however, that if the hadronic vacuum polarization determination using τ decay data turn out to be correct, then the HB/FP region will appear in a more favorable light!

Reach of LHC and LC in Dark Matter Allowed Regions of the mSUGRA Model

The reach of the CERN LHC for SUSY in the mSUGRA model has been calculated in Ref. [86] assuming 100 fb^{-1} of integrated luminosity. Briefly, sparticle pair production events were generated for many mSUGRA model parameter choices in the m_0 *vs.* $m_{1/2}$ plane for various $\tan\beta$ values. A fast LHC detector simulation (CMSJET) was used, and cuts were imposed to extract signal rates in a variety of multilepton plus multijet plus missing transverse energy channels. Backgrounds were also calculated from a variety of QCD and vector boson production processes. A large set of selection cuts were used to give some optimization over broad regions of parameter space. It was required to have at least a 5σ signal over background, with at least 10 signal events in the sample.

The reach of the CERN LHC is shown in Fig. 7 for the case of $\tan\beta = 30$ (55) left (right), $\mu > 0$, $A_0 = 0$ and $m_t = 175$ GeV. The dark shaded (red) regions are disallowed by lack of radiative electroweak symmetry breaking (REWSB) (right hand side) or presence of a stau LSP (left hand side). The light gray (yellow) region is excluded by LEP2 chargino searches ($m_{\tilde{\chi}^+} > 103.5$ GeV), while the region below the yellow contour gives $m_h < 114.4$ GeV, in contradiction of LEP2 SM Higgs searches (here, the SUSY h Higgs boson is essentially SM-like). The medium gray (green) regions have $\Omega_{CDM} h^2 < 0.129$, and are *allowed* by WMAP. The broad HB/FP region is seen on the right-hand side, while the stau co-annihilation region is shown on the left-hand side. At the edge of the LEP2 excluded region is the light Higgs annihilation corridor. The reach of the Fermilab Tevatron via the trilepton channel is also shown [87], assuming a 5σ signal over background for 10 fb^{-1}. The reach of the CERN LHC for 100 fb^{-1} of integrated luminosity is shown by the contour labeled "LHC". It extends from $m_{1/2} \sim 1400$ GeV (corresponding to a value of $m_{\tilde{g}} \sim 3$ TeV) on the left-hand side, to $m_{1/2} \sim 700$ GeV (corresponding to $m_{\tilde{g}} \sim 1.8$ TeV) on the right-hand side. In particular, for those values of $\tan\beta$, the LHC reach covers the entire stau co-annihilation region, plus the low $m_{1/2}$ portion of the HB/FP region. The outer limit of the reach contour is mainly determined by events in the $E_T^{miss}+$ jets channel, which arises from gluino and squark pair production, followed by hadronic cascade decays.

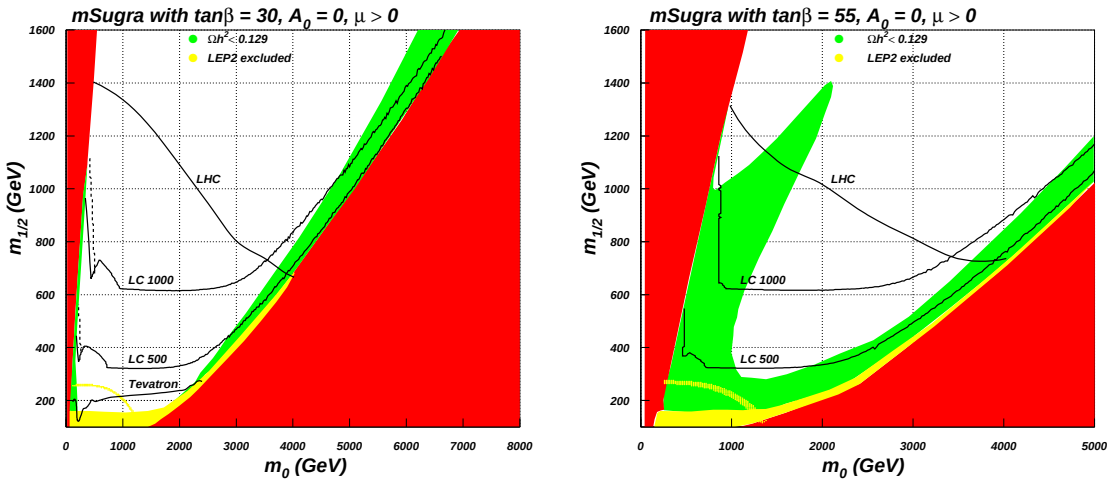


FIGURE 7. Parameter space of mSUGRA model for $\tan\beta = 30(55)$left(right), $A_0 = 0$ and $\mu > 0$, showing the reach of the Fermilab Tevatron, the CERN LHC and a 0.5 and 1 TeV linear e^+e^- collider for supersymmetry discovery.

We also show in the plot the reach of a $\sqrt{s} = 500$ and 1000 GeV LC, assuming 100 fb^{-1} of integrated luminosity [88]. Events were generated using Isajet 7.69, and compared against various SM backgrounds. The left-most portion of the reach contour arises where selectron and smuon pair production are visible, while the main portion (flat with $m_{1/2}$) arises due to chargino pair searches. An additional reach is gained between these two regions by searching for $e^+e^- \to \tilde{\chi}_2^0\tilde{\chi}_1^0$ production, followed by $\tilde{\chi}_2^0 \to \tilde{\chi}_1^0 b\bar{b}$ decay. In addition, in Ref. [89], additional reach can be gained by searching for stau pair events, although two photon backgrounds must be accounted for, due to the low energy release in the stau co-annihilation region.

While a 500 GeV LC can cover only a portion of the stau co-annihilation region, a 1 TeV LC can cover the entire region, at least for this value of $\tan\beta$. As one moves into the HB/FP region, the LC retains a significant reach for SUSY, which in fact extends *beyond* that of the CERN LHC! It is significant that this additional reach occurs in a DM allowed region of parameter space. In the HB/FP region, the superpotential μ parameter becomes small, and the lightest chargino and neutralino become increasingly light, with increased higgsino content. In fact, the decreasing mass gap between $\tilde{\chi}_1^+$ and $\tilde{\chi}_1^0$ makes chargino pair searches difficult at a LC using conventional cuts because there is so little visible energy release from the chargino decays. In Ref. [88, 89], we advocated cuts that pick out low energy release signal events from SM background, and allow a LC reach for chargino pairs essentially up to the kinematic limit for their production. In this case, it is important to fully account for $\gamma\gamma \to f\bar{f}$ backgrounds, where f is a SM fermion.

The case study of Ref. [88] also examined the HB/FP region with parameters $m_0 =$ 2500 GeV, $m_{1/2} = 300$ GeV, $A_0 = 0$, $\tan\beta = 30$, $\mu > 0$ and $m_t = 175$ GeV, *i.e.* in the HB/FP region. In this case, chargino pair events were selected from the 1ℓ+jets $+E_T^{miss}$ channel, and the dijet mass distribution was used to extract the value of $m_{\tilde{\chi}_1^+}$ and $m_{\tilde{\chi}_1^0}$ at the 10% level. The mass resolution is somewhat worse than in previous case studies

in the literature because the charginos undergo three-body rather than two-body decays, and no sharp edges in energy distributions are possible. Nonetheless, the measured value of chargino and neutralino mass, along with a measure of the total chargino pair cross section, was enough to determine the SUSY parameters M_2 and μ to 10-20% precision. The results, shown in Fig. 8, demonstrate that $\mu < M_2$, which points to a $\tilde{\chi}_1^+$ and $\tilde{\chi}_1^0$ which are higgsino/gaugino mixtures, as is characteristic of the HB/FP region.

In conclusion to this section, one should stress that the CERN LHC and an e^+e^- LC are highly complementary to each other in exploring the dark matter allowed parameter space of the mSUGRA model. LHC covers the stau co-annihilation region (completely for $\tan\beta < 40$) as well as the H, A funnel region (much of which is typically beyond the maximum reach of a LC). However only the lower part of the HB/FP region can be covered by the LHC. On the other hand, as we have demonstrated, LCs can probe much of the *upper* part of the HB/FP region with the new proposed cuts. Therefore, the combination of the LHC and a TeV scale LC can cover almost the entire parameter space of the mSUGRA scenario.

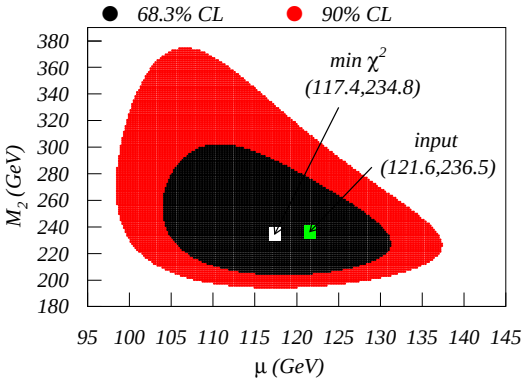


FIGURE 8. Determination of SUSY parameters from examining chargino pair production at a $\sqrt{s} = 0.5$ TeV LC, for the HB/FP mSUGRA point listed in the text.

Direct and Indirect CDM searches

Besides collider experiments there exist both direct and indirect non-accelerator dark matter search experiments, which are ongoing and proposed. Those experiments as will be discussed below play crucial role in restricting SUSY parameter space.

Direct CDM search experiments are aimed to look at neutral dark matter candidates scattering off nuclei. Direct dark matter detection has been recently examined by many authors [90], and observable signal rates are generally found in either the bulk annihilation region, or in the HB/FP region, while direct detection of DM seems unlikely in the A-funnel or in the stau co-annihilation region. Early limits on the spin-independent neutralino-nucleon cross-section (σ_{SI}) have been obtained by the CDMS [91], EDELWEISS [92] and ZEPLIN1 [93] groups, while a signal was claimed by the DAMA collaboration [94]. Collectively, we will refer to the reach from these groups as the "Stage 1" dark matter search. Depending on the neutralino mass, the combined limit on σ_{SI} varies from 10^{-5} to 10^{-6} pb. This cross section range is beyond the predicted levels from most supersymmetric models. However, experiments in the near future like CDMS2, CRESST2 [95], ZEPLIN2 and EDELWEISS2 (Stage 2 detectors) should have a reach of the order of 10^{-8} pb. In fact, the first results from CDMS2 have recently appeared, and yield a considerable improvement over the above mentioned Stage 1 results [96]. Finally, a number of experiments such as GENIUS [97], ZEPLIN4 [98] and XENON [99] are in the planning stage. We refer to these as Stage 3 detectors, which promise impressive limits of the order of $\sigma_{SI} < 10^{-9} - 10^{-10}$ pb, and would allow the exploration of a considerable part of parameter space of many supersymmetric models.

In particular, the Stage 3 direct DM detectors should be able to probe almost the entire HB/FP region of mSUGRA model parameter space. We note here in addition that the Warm Argon Program (WARP) [100] promotes a goal of detecting neutralino-nucleus scattering cross sections as low 10^{-11} pb.
Indirect detection of neutralino dark matter may occur via (for review, see *e.g.* [101, 102, 103]

1. observation of high energy neutrinos originating from $\widetilde{Z}_1\widetilde{Z}_1$ annihilations in the core of the sun or earth
2. observation of γ-rays originating from neutralino annihilation in the galactic core or halo and
3. observation of positrons or anti-protons originating from neutralino annihilation in the galactic halo.

The latter signals would typically be non-directional due to the influence of galactic magnetic fields, unless the neutralino annihilations occur relatively close to earth in regions of clumpy dark matter. The indirect signals for SUSY dark matter have been investigated in a large number of papers, and computer codes which yield the various signal rates are available [104, 47]. Recent works find that the various indirect signals occur at large rates in the now disfavored bulk annihilation region, and also in the HB/FP region [105, 106]. In Ref. [107], it was pointed out that the *A* annihilation funnel can give rise to large rates for cosmic γs, e^+s and $\bar{p}$s. However, neutralino-nucleon scattering cross sections are low in the *A* annihilation funnel, so that no signal is expected at neutrino telescopes, which depend more on the neutralino-nucleus scattering cross section than on the neutralino annihilation rates.

There is a bunch of various experiments for indirect dark matter detection. **Neutrino telescopes** such as Antares or IceCube are aimed to detect muon neutrinos from neutralino annihilation in the core of the earth or sun via $\nu_\mu \to \mu$ conversions. The Antares ν telescope should be sensitive to $E_\mu > 10$ GeV; it is in the process of deployment and is expected to turn on in 2006 [108]. It should attain a sensitivity of $100-1000$ μs/km^2/yr. The IceCube ν telescope is also in the process of deployment at the south pole [109, 110]. It should be sensitive to $E_\mu > 25-50$ GeV, and is expected to attain a sensitivity of $10-100$ μs/km^2/yr. Full deployment of all detector elements is expected to be completed by 2010.

Neutralino could also annihilate in the galactic halo giving rise **gamma rays, positrons or anti-protons** fluxes. The γ rays can be detected down to sub-GeV energies with space-based detectors such as EGRET [111] or GLAST [112]. Ground based arrays require much higher photon energy thresholds of order $20-100$ GeV. Experiments such as GLAST should be sensitive to rates of order 10^{-10} γs/cm^2/sec assuming $E_\gamma > 1$ GeV. In fact, it has recently been suggested that the extra-galactic gamma ray background radiation as measured by EGRET is well fit by a model of neutralino annihilation [113, 114]. In [115] detailed study has been done explaining not only the rate of SUSY contribution to the EGRET data but also the shape of various distribution through the non-trivial shape of CDM halo.

Positrons would arise as decay products of heavy quarks, leptons and gauge bosons produced in neutralino annihilations. Space based anti-matter detectors such as

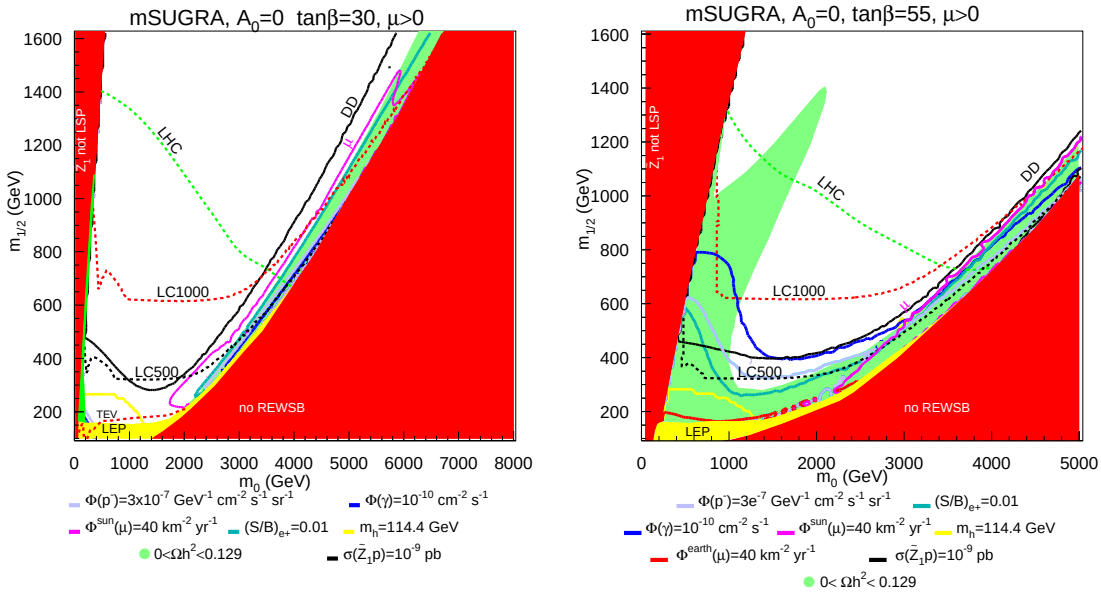


FIGURE 9. A plot of the reach of direct, indirect and collider searches for neutralino dark matter in the m_0 *vs.* $m_{1/2}$ plane, for $A_0 = 0$, $\tan\beta = 30(55)$left(right) and $\mu > 0$

Pamela [116] and AMS-02 [117] will be able to search for anomalous positron production from dark matter annihilation. The cosmic positron excess as measured by HEAT [118] has been suggested as having a source in galactic halo neutralino annihilations [119, 114]. It is suggested by Feng *et al.* [105, 106] that a reasonable observability criteria is that signal-to-background (S/B) rates should be greater than the 1-2% level. To calculate the S/B rates, we adopt fit C from Ref. [105, 106] for the $E^2 d\Phi_{e^+}/d\Omega dE$ background rate:

$$E^2 d\Phi_{e^+}/d\Omega dE = 1.6 \times 10^{-3}\, E^{-1.23}, \tag{16}$$

where E is in GeV.

Anti-protons may also be produced in the debris of neutralino annihilations in the galactic halo. Such anti-protons have been measured by the BESS collaboration [120]. The differential flux of anti-protons from the galactic halo, $d\Phi_{\bar{p}}/dE_{\bar{p}}d\Omega$, as measured by BESS, has a peak in the kinetic energy distribution at $E_{\bar{p}} \sim 1.76$ GeV. The height of the peak at $E_{\bar{p}} \sim 1.76$ GeV is $\sim 2 \times 10^{-6}$ $\bar{p}$/GeV/cm^2/s/sr. Signal rates in the range of $10^{-7} - 10^{-6}$ $\bar{p}$/GeV/cm^2/s/sr might thus provide a benchmark for observability.

Our results for direct/indirect DM search experimental reach for the mSUGRA model are shown in Fig. 9 in the m_0 *vs.* $m_{1/2}$ plane for $\tan\beta = 30$ and 55 (left and right respectively), $A_0 = 0$ and $\mu > 0$. If addition to collider reach presented in the previous figures, here w e show contours of

- Stage 3 direct detection experiments ($\sigma_{SI} > 10^{-9}$ pb; black contour),
- reach of IceCube ν telescope with $\Phi^{sun}(\mu) = 40$ μs/km^3/yr and $E_\mu > 25$ GeV (magenta contour),

- the $\Phi(\gamma) = 10^{-10}$ γs/cm^2/s contour with $E_\gamma > 1$ GeV in a cone of 0.001 sr directed at the galactic center (dark blue contour),
- the $S/B > 0.01$ contour for halo produced positrons (blue-green contour) and
- the anti-proton flux rate $\Phi(\bar{p}) = 3 \times 10^{-7}$ $\bar{p}$s/cm^2/s/sr (lavender contour).

As noted by Feng *et al.* [105, 106], *all* these indirect signals are visible inside some portion of the HB/FP region, while *none* are visible in generic DM disallowed regions (under the assumed smooth halo profiles). The intriguing point is that almost the entire HB/FP region can be explored by the cubic km scale IceCube ν telescope! It can also be explored (apparently at later times) by the Stage 3 direct DM detectors. Taking into account relative time scales of the various search experiments, if SUSY lies within the upper HB/FP region, then it could be discovered first by IceCube (and possibly Antares), with a signal being later confirmed by direct DM detection and possibly by the TeV scale linear e^+e^- collider. There is also some chance to obtain indirect γ, e^+ and $\bar{p}$ signals in this region. Notice that if instead SUSY lies within the stau co-annihilation corridor, then it will be discovered by the LHC, but all indirect detection experiments will find null results in their DM searches.

BEYOND MSUGRA: NORMAL MASS HIERARCHY

We see that Δa_μ favors light second-generation sleptons, while $BF(b \to s\gamma)$ prefers heavy third generation squarks. Since this situation is hard to realize in the mSUGRA model, this could be an indication that one must move beyond the assumption of universality, wherein each generation has a common mass at $Q = M_{GUT}$. Therefore scenario in which first and second generation scalars remain degenerate, while allowing for a significant splitting with third generation scalars is well motivated. In this case, heavy (multi-TeV) third generation scalars are preferred by $BF(b \to s\gamma)$ constraints, while rather light first and second generation scalars are preferred by Δa_μ. The scenario is called the normal scalar mass hierarchy (NMH). The parameter set of the mSUGRA model is expanded to the following values: [85]

$$m_0(1),\ m_0(3),\ m_H,\ m_{1/2},\ A_0,\ \tan\beta,\ sign(\mu). \tag{17}$$

where $m_0(1)$ is the common scalar mass of all *first and second* generation scalars at $Q = M_{GUT}$, while $m_0(3)$ is the common mass of all *third* generation scalars at M_{GUT}. The above parameter set is well motivated in $SO(10)$ SUSY GUT models, where the two MSSM Higgs doublets typically occupy a **10** of $SO(10)$, and each generation of scalars, along with a SM gauge singlet N occupies the **16** dimensional spinorial representation of $SO(10)$. The step of breaking generational universality must be taken with some caution, since in general it can lead to violations of constraints from FCNC processes. Splitting the third generation from the first and second can potentially lead to violations of FCNC processes. One of the main experimentally measured bounds on FCNC processes in this case comes from $B_H^0 - B_L^0$ mass splitting. One can show that Δm_B is much less restrictive than the kaon case, for both low and high squark masses. Moreover, even if squark mass

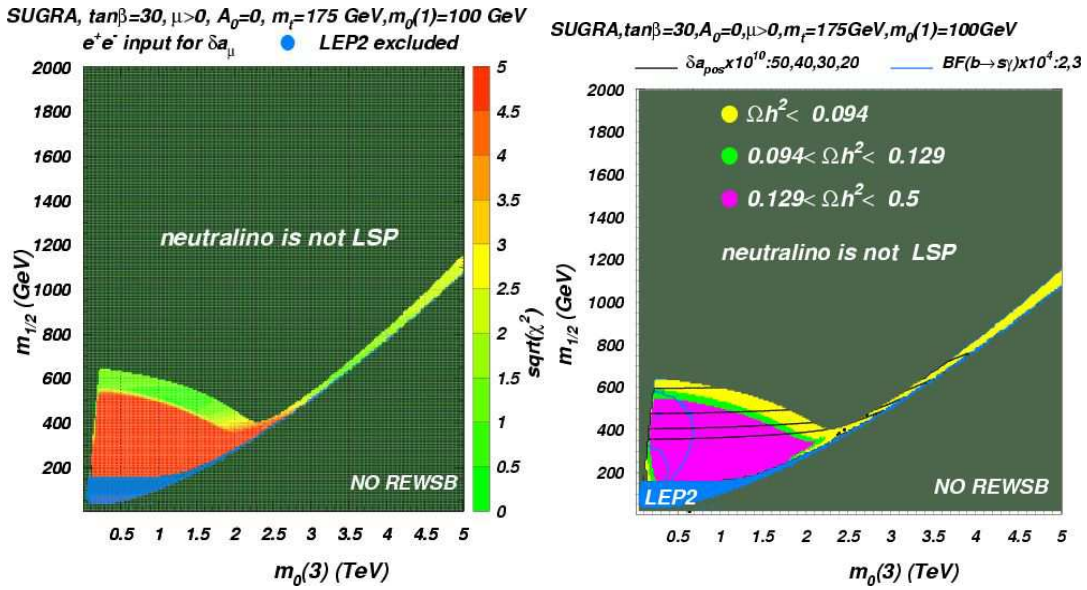


FIGURE 10. Left frame: $\sqrt{\chi^2}$ values in the $m_0(3)$ *vs.* $m_{1/2}$ plane for $m_0(1) = 100$ GeV, $\tan\beta = 30$, $A_0 = 0$ and $\mu > 0$ in NMH SUGRA scenario.The green regions have low χ^2, while red regions have high χ^2. Yellow is intermediate. Right frame: constraints for NMH SUGRA model in the $m_0(3)$ vs. $m_{1/2}$ plane for $m_0(1) = 100$GeV, $A_0 = 0$ and $\tan\beta = 30$. Allowed CDM relic density regions are the green shaded ones, LEP2 excluded regions denoted by blue color. Black contours denotes δa_μ values $(30, 10, 5, 1 \times 10^{-10}$ – from bottom to top) and blue contours denote $BF(b \to s\gamma)$ values ($2, 3 \times 10^{-4}$ – from bottom to top). The bottom raw of figures presents $\sqrt{\chi^2}$ for the respective parameters of the mSUGRA model

splittings are very large at the scale $Q = M_{GUT}$, the weak scale mass splittings are much smaller and practically whole parameter space of NMH SUGRA is allowed [85].

Scan in the SUGRA parameter space of Eq. 17 and respective χ^2 analysis show the following preferences [85]: $m_H \sim m_0(3)$, $m_0(1) \ll m_0(3)$, $m_0(1) \sim 0 - 400$ GeV, $m_0(3) \sim 500 - 3000$ and large $m_0(1) - m_0(3)$ mass splitting and that mainly large $\tan\beta$ is preferred if the generational mass splitting is small (which takes us back towards the mSUGRA case). If may also be pointed out that SUSY IMH models are greatly disfavored. The above scan motivates to reduce the number of parameters and choose $m_H = m_0(3)$ which brings us to the minimal extension of mSUGRA space by just one additional parameter $m_0 \to [m0(1), m_0(3)]$. In Fig. 10(left) we present the $\sqrt{\chi^2}$ values in the $m_0(3)$ *vs.* $m_{1/2}$ plane for $m_0(1) = 100$ GeV, $\tan\beta = 30$, $A_0 = 0$ and $\mu > 0$. The corresponding contour plots of $BF(b \to s\gamma)$, a_μ and Ωh^2 are shown in right frame of the figure. One can see that most of the area displayed is excluded. In this case, slepton masses are quite light, in the vicinity of a few hundred GeV. As $m_{1/2}$ increases, ultimately $m_{\tilde{Z}_1}$ becomes greater than $m_{\tilde{\ell}}$, and one violates the cosmological constraint on stable charged relics from the Big Bang. On the other hand, of the *surviving* parameter space, there are large regions with relatively low χ^2. The plot with $m_0(1) =$ 100 GeV has a rather broad band of low χ^2. In this case, neutralinos in the early universe can annihilate by a combination of t-channel slepton exchange (as in the bulk

region of mSUGRA), and by neutralino-slepton co-annihilation. In addition, smuons and mu sneutrinos are relatively light, giving a large, positive contribution to Δa_μ, while top squarks inhabit the TeV and beyond range, effectively suppressing anomalous contributions to $BF(b \to s\gamma)$. In addition to the region with low values of $m_0(3)$ and low $m_{1/2}$, an important portion the HB/FP region survives since low $m_0(1)$ value provides big enough contribution to Δa_μ while big $m_0(3)$ value keeps SUSY contribution to $BR(b \to s\gamma)$ suppressed.

The scenario of NMH SUGRA model works if $m_0(1) \simeq m_0(2) \ll m_0(3)$, and leads to spectra typically with squarks and third generation sleptons in the TeV range, while first and second generation sleptons have masses in the range of 100-300 GeV. The presence of rather light first and second generation sleptons in the sparticle mass spectrum in general leads to enhancements in leptonic cross sections from superparticle production at collider experiments, compared to the case where selectrons and smuons are in the multi-TeV range — sleptons may now be produced with non-negligible cross sections at colliders, and also in that their presence enhances the leptonic branching fractions of charginos and especially neutralinos. Therefore it is worth to discuss the implications of light selectrons and smuons for the Fermilab Tevatron collider, the CERN LHC and a linear e^+e^- collides.

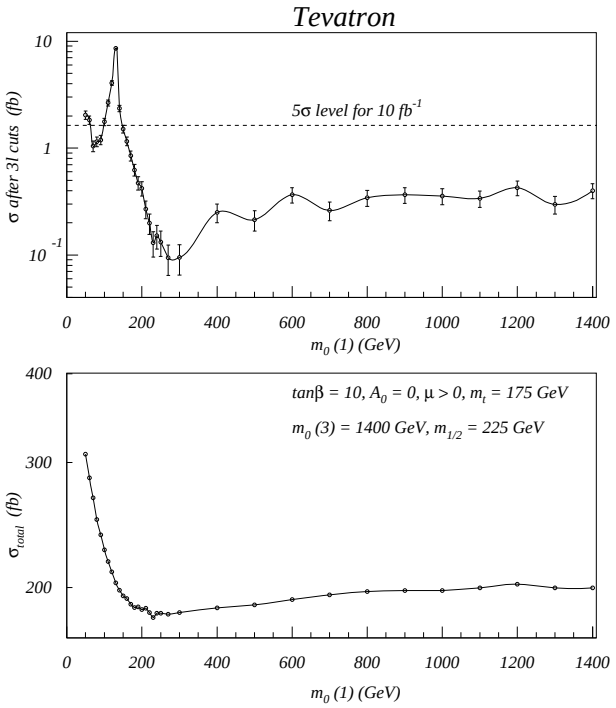


FIGURE 11. Rates for isolated trilepton events at the Fermilab Tevatron $p\bar{p}$ collider, after cuts SC2 from Ref. [121, 122, 123]

It is usually expected that $p\bar{p} \to \widetilde{W}_1^+ \widetilde{W}_1^- X$ and $\widetilde{W}_1 \widetilde{Z}_2 X$ will be the dominant production cross sections [55] at the Tevatron if sparticle are accessible. If $\widetilde{W}_1 \to \ell \nu_\ell \widetilde{Z}_1$ and $\widetilde{Z}_2 \to \ell\ell\widetilde{Z}_1$, then clean trilepton signals may occur at an observable rate. Signal and background rates have recently been investigated in Ref. [121, 122, 123], where Tevatron reach plots may also be found.

Fig. 11 presents isolated trilepton Isajet 7.69 signal after using cuts SC2 of Ref. [122], where the backgrounds are also evaluated for for the parameter space point $m_0(3) =$ 1400 GeV, $m_{1/2} = 225$ GeV, $A_0 = 0$, $\tan\beta = 10$ and $\mu > 0$. The results are plotted versus variation in the $m_0(1)$ parameter, the signal level needed for a 5σ signal with 10 fb^{-1} is also denoted. The error bars show the Monte Carlo statistical error. When $m_0(1) = m_0(3)$ (at $m_0(1) = 1400$ GeV), the results correspond to the mSUGRA model, and the isolated trilepton signal is well below discovery threshold. At $m_0(1) \lesssim 200$ GeV (which is favorable by δa_μ data) the light sleptons begin to dominate neutralino three

body decays rates, and consequently the trilepton cross section rises steeply, to the level of observability. Eventually chargino and and neutralino two-body decays to sleptons turn on (in this case, first $\widetilde{Z}_2 \to \tilde{\ell}_R \ell$), and trilepton rates become very high.

Similarly, at the the CERN LHC, $m_0(1)$ drops below about 200 GeV (the value typically needed to explain the $(g-2)_\mu$ anomaly), multilepton rates rise steeply. Thus, we would expect that SUSY – as manifested in the NMH SUGRA model – would be easily discovered, and what's more, the signal events would be unusually rich in multilepton events. Such multilepton events can be especially useful for reconstructing sparticle masses in gluino and squark cascade decay events [124].

A linear collider operating at $\sqrt{s} = 0.5 - 1$ TeV may be the next frontier particle physics accelerator beyond the CERN LHC. Depending on sparticle masses and the collider energy, charginos and neutralinos may or may not be accessible. However, in the NMH SUGRA model, light first and second generation sleptons are needed both to explain the $(g-2)_\mu$ anomaly, but also to enhance neutralino annihilation in the early universe. This means slepton masses are typically in the 100-300 GeV range, and likely within reach of a linear e^+e^- collider [88].

SUSY GUTS AND YUKAWA UNIFIED SUSY MODELS

The existence of the weak scale supersymmetry leads to gauge coupling unification at the scale of $M_{GUT} \simeq 2^{16}$ GeV which in its turn is compelling hing for SUSY grand unified theories or SUSY GUTs. Such a SUSY GUT theory may be the "low energy effective theory" that can be obtained from some more fundamental superstring theory. Models based on the gauge group $SU(5)$ are compelling in that they explain the apparently ad-hoc hypercharge assignments of the SM fermions [125, 126, 127]. However, many $SU(5)$ SUSY GUT models as formulated in four dimensions are already excluded by proton decay constraints [128]. $SU(5)$ SUSY GUT models can also be formulated in five or more dimensions, where compactification of the extra dimensions leads to a break down in gauge symmetry [129, 130, 131, 132, 133]. These models can dispense with the unwieldy large Higgs representations required by four-dimensional models, and can also be constructed to suppress or eliminate proton decay entirely.

Further step to the complete gauge and matter field family unification (as well as Yukawa coupling unification as we discuss below) can be achieved in SUSY GUTs models based on SO(10) group which therefore looks very intriguing [134, 135, 136, 137, 138]. In addition to unifying gauge couplings,

- They unify all matter of a single generation into the 16 dimensional spinorial multiplet of $SO(10)$.
- The **16** of $SO(10)$ contains in addition to all SM matter fields of a single generation a gauge singlet right handed neutrino state which naturally leads to a mass for neutrinos. The well-known see-saw mechanism [139, 140, 141] implies that if $m_{\nu_\tau} \sim 0.03$ eV, as suggested by atmospheric neutrino data [142, 143], then the mass scale associated with ν_R is very close to the GUT scale: *i.e.* $M_N \sim 10^{15}$ GeV.

- $SO(10)$ explains the apparently fortuitous cancellation of triangle anomalies within the SM.
- The structure of the neutrino sector of $SO(10)$ models lends itself to a successful theory of baryogenesis via intermediate scale leptogenesis (For a review, see [144].
- In the simplest $SO(10)$ SUSY GUT models, the two Higgs doublets of the MSSM occupy the same 10 dimensional Higgs multiplet $\phi(\mathbf{10})$. The superpotential then contains the term $\hat{f} \ni f\hat{\psi}(\mathbf{16})\hat{\psi}(\mathbf{16})\hat{\phi}(\mathbf{10}) + \cdots$ where f is the single Yukawa coupling for the third generation. Thus, the simplest $SO(10)$ SUSY GUT models predict $t-b-\tau$ Yukawa coupling unification in addition to gauge coupling unification.

It is possible to calculate the t, b and τ Yukawa couplings at $Q = m_{weak}$, and extrapolate them to M_{GUT} in much the same way one checks the theory for gauge coupling unification. Yukawa coupling unification turns out to depend on the entire spectrum of sparticle masses and mixings since these enter into the weak scale supersymmetric threshold corrections. Thus, the requirement of $t-b-\tau$ Yukawa coupling unification can be a powerful constraint on the soft SUSY breaking terms of the low energy effective theory [145, 146, 147, 148, 149, 150].

In Ref. [151], it was found that models with Yukawa coupling unification with $R < 1.05$ (good to 5%) could be found if additional D-term splittings of scalar masses were included. Here, $R \equiv max(f_t,\ f_b,\ f_\tau)/min(f_t,\ f_b,\ f_\tau)$, where all Yukawa couplings are evaluated at the GUT scale. The D-term splittings occur naturally when the $SO(10)$ gauge symmetry breaks to $SU(5)$, and they are given by (see [152] and references in it).

$$\begin{aligned} m_Q^2 = m_E^2 = m_U^2 &= m_{16}^2 + M_D^2, \\ m_D^2 = m_L^2 &= m_{16}^2 - 3M_D^2, \\ m_N^2 &= m_{16}^2 + 5M_D^2, \\ m_{H_{u,d}}^2 &= m_{10}^2 \mp 2M_D^2, \end{aligned} \tag{18}$$

where M_D^2 parameterizes the magnitude of the D-terms. Owing to our ignorance of the gauge symmetry breaking mechanism, M_D^2 can be taken as a free parameter, with either positive or negative values. $|M_D|$ is expected to be of order the weak scale. Thus, the D-term (DT) model is characterized by the following free parameters,

$$m_{16},\ m_{10},\ M_D^2,\ m_{1/2},\ A_0,\ \tan\beta,\ \mathrm{sign}(\mu). \tag{19}$$

Using the DT model, Yukawa unification good to 5% was found when soft term parameters m_{16} and m_{10} were scanned up to 1.5 TeV, but only for $\mu < 0$ values [151, 59]. The essential quality of the D-term mass splitting is that it gave the value of m_{H_u} a head start over m_{H_d} in running towards negative values, as is required for REWSB. Good relic density was also found in the stau co-annihilation and hyperbolic branch/focus point (HB/FP) region, but at some cost to the degree of Yukawa coupling unification.

In Ref. [153], it was found that Yukawa coupling unification good to only 30% could be achieved in DT models with $\mu > 0$ when m_{16} values were scanned up to 2 TeV. The models with the best Yukawa coupling unification were found to have soft term relations

$$A_0^2 \simeq 2m_{10}^2 \simeq 4m_{16}^2, \tag{20}$$

which had also been found by Bagger *et al.* in the context of radiatively driven inverted scalar mass hierarchy (IMH) models [154, 155, 156, 157, 158, 159].

In Ref. [153], a model with just GUT scale Higgs mass splittings was also examined (*HS*), while all other scalars remained universal.

The parameter space of the *HS* model is that of Eq. 19, but where the *D*-term splitting is only applied to the last of the relations in Eq. 18. Yukawa coupling unification in the *HS* model was found to be comparable to the *DT* model case when m_{16} values up to 2 TeV were scanned. In Ref. [160] (Auto *et al.*), soft term values of m_{16} up to 20 TeV were explored. In this case, Yukawa unified solutions to better than 5% were found for $\mu > 0$ for the *HS* model when very large values of $m_{16} > 5-10$ TeV were scanned. The large scalar masses that gave rise to Yukawa unification also acted to suppress neutralino annihilation in the early universe, so that rather large values of the relic density were found. Models with $\Omega_{\widetilde{Z}_1} h^2 < 0.2$ could be found, but only at the expense of accepting Yukawa coupling unification to 20%, rather than 5%. The models found with low relic density generally had either a low μ value, or were in the light Higgs annihilation corridor, with $2m_{\widetilde{Z}_1} \sim m_h$.

Similar work has been carried on by Blazek, Dermisek and Raby (BDR). In Ref. [161, 162], the BDR group used a top-down approach to the RG sparticle mass solution to find Yukawa unified solutions for $\mu > 0$, where they also noted that in this case the *HS* model worked better than the *DT* model. In their approach, the third generation fermion masses and other electroweak observables were an output of the program, so that starting with models with perfect Yukawa coupling unification, they would look for solutions with a low χ^2 value constructed from the low energy observables. The BDR Yukawa unified solutions were also characterized by soft term IMH model boundary conditions. The solutions differed from those of Ref. [160] in that they always gave a very low value of Higgs mass m_A and also small μ parameter, indicative of a mixed higgsino-bino LSP. In Ref. [163], the neutralino relic density was examined for the BDR solutions. Their low μ and m_A values generally led to very low values of $\Omega_{\widetilde{Z}_1} h^2$ unless $m_{1/2}$ was small enough compared to μ that the LSP was in the mixed higgsino-bino region.

Finally, one more step was done in [152] to solve the problem of tension between Yukawa unification and low relic density in SO(10) SUSY GUTs models. In this paper, two methods were explored to reconcile Yukawa unified sparticle mass solutions with the neutralino relic density. The first case is to allow splitting of the third generation of scalars from the first two generations. By decreasing the first and second generation scalar masses, sparticle mass solutions with very light $\tilde{u}_R$ and $\tilde{c}_R$ squark masses, in the 90-120 GeV range were obtained. The other examined scenario was the case of non-degenerate gaugino masses at the *GUT* scale. Beginning with any of the Yukawa unified solutions found in an earlier study, it was found that by dialing M_1 to large enough values, a (partially) wino-like LSP can be generated, with a relic density in accord with WMAP allowed values.

In Fig. 12, we show the example of such solution for the first scenario in the $m_{16}(1)$ *vs.* $m_{1/2}$ plane for fixed $m_{16}(3) = 7826.5$ GeV. The blue region at low $m_{1/2}$ is excluded by the LEP2 bound on chargino mass $m_{\widetilde{W}_1} > 103.5$ GeV. The black region on the left is excluded because the $m^2_{U_1}$ squared mass is driven tachyonic, resulting in a color symmetry violating ground state. The green region denotes sparticle mass spec-

trum solution with relic density $0.094 < \Omega_{\tilde{Z}_1} h^2 < 0.129$, within the WMAP favored regime, while the yellow region denotes even lower relic density values, wherein the CDM in the universe might be a mixture of neutralinos plus some other species. The red region has $\Omega_{\tilde{Z}_1} h^2 < 0.5$. The remaining unshaded regions give sparticle spectra solutions with $\Omega_{\tilde{Z}_1} h^2 > 0.5$, and would be excluded by WMAP. We also show several contours of $BF(b \to s\gamma)$, Δa_μ^{SUSY} and R, the max/min ratio of GUT scale Yukawa couplings. We see that all constraints on the sparticle mass spectrum are within allowable limits for the shaded region to the right of the excluded region.

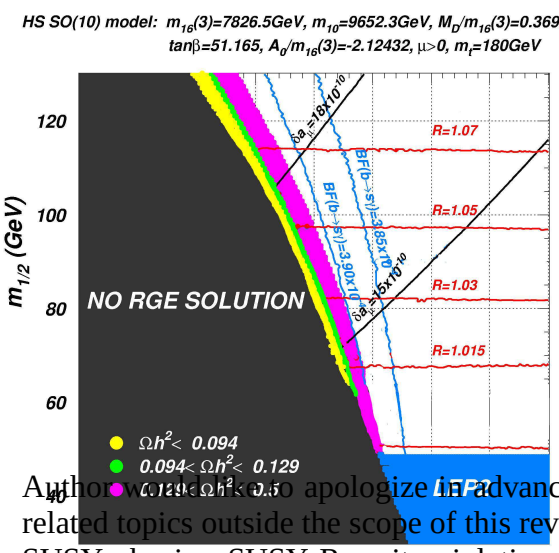


FIGURE 12. Allowed parameter space of Yukawa unified supersymmetric HS model with generational non-universality from [152]. We show the $m_{16}(1)$ *vs.* $m_{1/2}$ plane for $m_{16}(3) = 7830$ GeV, $m_{10} = 9650$ GeV, $M_D/m_{16}(3) = 0.37$, $A_0/m_{16}(3) = -2.1$, $\mu > 0$, $\tan\beta = 51$ and $m_t = 180$ GeV. The black-shaded region gives tachyonic particles, while the blue region is excluded by LEP2 chargino search experiments. The yellow and green regions are allowed by the WMAP determination of $\Omega_{\tilde{Z}_1} h^2$. We also show contours of $BF(b \to s\gamma)$, the measure of Yukawa unification at M_{GUT}.

The origin of the light squarks comes from the S term in the one-loop RGEs, which is non-zero and large in the case of multi-TeV valued split Higgs masses. A search for just two light squarks at the Fermilab Tevatron collider using the new Run 2 data should be able to either verify or disprove this scenario. In addition, the light squarks give rise to large rates for direct detection of dark matter, and should give observable rates for searches at CDMS II.

CONCLUSIONS

Authors would also like to apologize in advance for leaving several other interesting SUSY related topics outside the scope of this review. Among them are CP and flavor violating SUSY physics, SUSY R-parity violation, beyond the MSSM (nMSSM) scenarios and various SUSY-related aspects of baryogenesis. There are also open fundamental problems, which still need to be solved. One of the most important problems is Cosmological constant problem and the problem of origin of the μ term.

The most of the attention in this review was paid to SUGRA models which are very compelling indeed. In constraining SUGRA parameter space CDM constraints play a crucial role leaving only a few restricted regions to be tested by other experiments. LEP2 $(b \Rightarrow s\gamma)$ + $(g_\mu - 2)$ constraints leave *focus point*, *funnel* and *stau-co-annihilation* region survived. LHC collider can uniquely cover the funnel region and (almost) all stau-co-annihilation region, but leaves most of the focus point region uncovered. On the other hand, NLC could greatly extend LHC reach in focus point region. There is also a great complementary role of direct and indirect DM search experiments which has the potential to cover completely focus point region leaving 'no escape' for mSUGRA with upcoming experiments combined!

There could be an indication coming from from δa_μ data that normal mass hierarchy in SUGRA scenario could be preferred by nature and that, may be, mSUGRA scenario is too simple to be true.

Talking about GUTs models, SO(10) SUSY GUTs looks very attractive from both, theoretical and phenomenological points of view, and predicts very specific particle spectra testable experimentally.

Finally, I would like to express my belief that the our exciting era of upcoming

experiments will be indeed successful in hunting for Supersymmetry which could be just around corner!

ACKNOWLEDGMENTS

Author would like to thank his FSU colleagues, Howie Baer, Daniel Auto, Azar Mustafayev, Jorge O'Farrill, Tadas Krupovnikas and Csaba Balazs for very fruitful collaboration. I am also grateful to Dmitri Kazakov, Alexei Gladyshev, Daisuke Nomura, Sekhar Shivukula, Elizabeth Simmons, Anatoly Solomin, Kazuhiro Tobe, Wu-Ki Tung and C.-P. Yuan for numerous stimulating discussions during the preparation of this review. DOE support is also acknowledged.

REFERENCES

1. Golfand, Y. A., and Likhtman, E. P., *JETP Lett.*, **13**, 323–326 (1971).
2. Ramond, P., *Phys. Rev.*, **D3**, 2415–2418 (1971).
3. Neveu, A., and Schwarz, J. H., *Phys. Rev.*, **D4**, 1109–1111 (1971).
4. Volkov, D. V., and Akulov, V. P., *Phys. Lett.*, **B46**, 109–110 (1973).
5. Wess, J., and Zumino, B., *Nucl. Phys.*, **B70**, 39–50 (1974).
6. Haag, R., Lopuszanski, J. T., and Sohnius, M., *Nucl. Phys.*, **B88**, 257 (1975).
7. Nath, P., and Arnowitt, R., *Phys. Lett.*, **B56**, 177 (1975).
8. Freedman, D. Z., van Nieuwenhuizen, P., and Ferrara, S., *Phys. Rev.*, **D13**, 3214–3218 (1976).
9. Deser, S., and Zumino, B., *Phys. Lett.*, **B62**, 335 (1976).
10. Muller-Kirsten, H. J. W., and Wiedemann, A., Supersymmetry: An introduction with conceptual and calculational details (1986), print-86-0955 (KAISERSLAUTERN).
11. Wess, J., and Bagger, J., Supersymmetry and supergravity (1992), princeton, USA: Univ. Pr. (1992) 259 p.
12. Drees, M., An introduction to supersymmetry (1996), hep-ph/9611409.
13. Lykken, J. D., Introduction to supersymmetry (1996), hep-th/9612114.
14. Martin, S. P., A supersymmetry primer (1997), hep-ph/9709356.
15. Polonsky, N., *Lect. Notes Phys.*, **M68**, 1–169 (2001).
16. Girardello, L., and Grisaru, M. T., *Nucl. Phys.*, **B194**, 65 (1982).
17. Chamseddine, A. H., Arnowitt, R., and Nath, P., *Phys. Rev. Lett.*, **49**, 970 (1982).
18. Barbieri, R., Ferrara, S., and Savoy, C. A., *Phys. Lett.*, **B119**, 343 (1982).
19. Hall, L. J., Lykken, J., and Weinberg, S., *Phys. Rev.*, **D27**, 2359–2378 (1983).
20. Dine, M., and Nelson, A. E., *Phys. Rev.*, **D48**, 1277–1287 (1993).
21. Dine, M., Nelson, A. E., and Shirman, Y., *Phys. Rev.*, **D51**, 1362–1370 (1995).
22. Dine, M., Nelson, A. E., Nir, Y., and Shirman, Y., *Phys. Rev.*, **D53**, 2658–2669 (1996).
23. Aguilar-Saavedra, J. A., et al., Tesla technical design report part iii: Physics at an e+e- linear collider (2001), hep-ph/0106315.
24. Randall, L., and Sundrum, R., *Nucl. Phys.*, **B557**, 79–118 (1999).
25. Giudice, G. F., Luty, M. A., Murayama, H., and Rattazzi, R., *JHEP*, **12**, 027 (1998).
26. Kaplan, D. E., Kribs, G. D., and Schmaltz, M., *Phys. Rev.*, **D62**, 035010 (2000).
27. Chacko, Z., Luty, M. A., Nelson, A. E., and Ponton, E., *JHEP*, **01**, 003 (2000).
28. Kaplunovsky, V. S., and Louis, J., *Phys. Lett.*, **B306**, 269–275 (1993).
29. Soni, S. K., and Weldon, H. A., *Phys. Lett.*, **B126**, 215 (1983).
30. Choi, K., Lee, J. S., and Munoz, C., *Phys. Rev. Lett.*, **80**, 3686–3689 (1998).
31. Paige, F. E., Protopescu, S. D., Baer, H., and Tata, X., Isajet 7.69: A monte carlo event generator for p p, anti-p p, and e+ e- reactions (2003), hep-ph/0312045.
32. Allanach, B. C., *Comput. Phys. Commun.*, **143**, 305–331 (2002).
33. Porod, W., *Comput. Phys. Commun.*, **153**, 275–315 (2003).

34. Djouadi, A., Kneur, J.-L., and Moultaka, G., Suspect: A fortran code for the supersymmetric and higgs particle spectrum in the mssm (2002), hep-ph/0211331.
35. Allanach, B. C., Kraml, S., and Porod, W., *JHEP*, **03**, 016 (2003).
36. W.Freedman, and M.Turner, *Rev. Mod. Phys.*, **75**, 1433 (2003).
37. Lahanas, A. B., Mavromatos, N. E., and Nanopoulos, D. V., *Int. J. Mod. Phys.*, **D12**, 1529–1591 (2003).
38. Spergel, D. N., et al., *Astrophys. J. Suppl.*, **148**, 175 (2003).
39. Bennett, C. L., et al., *Astrophys. J. Suppl.*, **148**, 1 (2003).
40. Goldberg, H., *Phys. Rev. Lett.*, **50**, 1419 (1983).
41. Ellis, J. R., Hagelin, J. S., Nanopoulos, D. V., Olive, K. A., and Srednicki, M., *Nucl. Phys.*, **B238**, 453–476 (1984).
42. Griest, K., and Seckel, D., *Phys. Rev.*, **D43**, 3191–3203 (1991).
43. Gondolo, P., and Gelmini, G., *Nucl. Phys.*, **B360**, 145–179 (1991).
44. Edsjo, J., and Gondolo, P., *Phys. Rev.*, **D56**, 1879–1894 (1997).
45. Baer, H., Balazs, C., and Belyaev, A., *JHEP*, **03**, 042 (2002).
46. Gondolo, P., Edsjo, J., Bergstrom, L., Ullio, P., and Baltz, E. A., Darksusy: A numerical package for dark matter calculations in the mssm (2000), astro-ph/0012234.
47. Gondolo, P., et al., Darksusy: A numerical package for supersymmetric dark matter calculations (2002), astro-ph/0211238.
48. Belanger, G., Boudjema, F., Pukhov, A., and Semenov, A., *Comput. Phys. Commun.*, **149**, 103–120 (2002).
49. Belanger, G., Boudjema, F., Pukhov, A., and Semenov, A., Micromegas: Version 1.3 (2004), hep-ph/0405253.
50. Ellis, J. R., Falk, T., and Olive, K. A., *Phys. Lett.*, **B444**, 367–372 (1998).
51. Ellis, J. R., Falk, T., Ganis, G., and Olive, K. A., *Phys. Rev.*, **D62**, 075010 (2000).
52. Chan, K. L., Chattopadhyay, U., and Nath, P., *Phys. Rev.*, **D58**, 096004 (1998).
53. Feng, J. L., Matchev, K. T., and Moroi, T., *Phys. Rev.*, **D61**, 075005 (2000).
54. Baer, H., Chen, C.-h., Paige, F., and Tata, X., *Phys. Rev.*, **D53**, 6241–6264 (1996).
55. Baer, H., Chen, C.-h., Paige, F., and Tata, X., *Phys. Rev.*, **D52**, 2746–2759 (1995).
56. Drees, M., and Nojiri, M. M., *Phys. Rev.*, **D47**, 376–408 (1993).
57. Baer, H., and Brhlik, M., *Phys. Rev.*, **D53**, 597–605 (1996).
58. Baer, H., and Brhlik, M., *Phys. Rev.*, **D57**, 567–577 (1998).
59. Baer, H., et al., *Phys. Rev.*, **D63**, 015007 (2001).
60. Ellis, J. R., Falk, T., Ganis, G., Olive, K. A., and Srednicki, M., *Phys. Lett.*, **B510**, 236–246 (2001).
61. Roszkowski, L., Ruiz de Austri, R., and Nihei, T., *JHEP*, **08**, 024 (2001).
62. (2004), joint LEP2 Supersymmetry Working Group, *Combined LEP Chargino Results, up to 208 GeV*, `http://lepsusy.web.cern.ch/lepsusy`.
63. (2004), joint LEP2 Supersymmetry Working Group, *Combined LEP Selectron/Smuon/Stau Results, 183-208 GeV*, `http://lepsusy.web.cern.ch/lepsusy`.
64. Group, L. H. W., Searches for the neutral higgs bosons of the mssm: Preliminary combined results using lep data collected at energies up to 209-gev (2001), hep-ex/0107030.
65. Abazov, V. M., et al., *Nature*, **429**, 638–642 (2004).
66. Abe, K., et al., *Phys. Lett.*, **B511**, 151–158 (2001).
67. Cronin-Hennessy, D., et al., *Phys. Rev. Lett.*, **87**, 251808 (2001).
68. Barate, R., et al., *Phys. Lett.*, **B429**, 169–187 (1998).
69. Ellis, J. R., Olive, K. A., and Santoso, Y., *New J. Phys.*, **4**, 32 (2002).
70. Djouadi, A., Drees, M., and Kneur, J. L., *JHEP*, **08**, 055 (2001).
71. Baer, H., and Brhlik, M., *Phys. Rev.*, **D55**, 3201–3208 (1997).
72. Baer, H., Brhlik, M., Castano, D., and Tata, X., *Phys. Rev.*, **D58**, 015007 (1998).
73. Degrassi, G., Gambino, P., and Giudice, G. F., *JHEP*, **12**, 009 (2000).
74. Carena, M., Garcia, D., Nierste, U., and Wagner, C. E. M., *Phys. Lett.*, **B499**, 141–146 (2001).
75. Bennett, G. W., et al., *Phys. Rev. Lett.*, **92**, 161802 (2004).
76. Bennett, G. W., et al., *Phys. Rev. Lett.*, **89**, 101804 (2002).
77. Davier, M., Eidelman, S., Hocker, A., and Zhang, Z., *Eur. Phys. J.*, **C31**, 503–510 (2003).
78. Hagiwara, K., Martin, A. D., Nomura, D., and Teubner, T., *Phys. Rev.*, **D69**, 093003 (2004).
79. Abe, F., et al., *Phys. Rev.*, **D57**, 3811–3816 (1998).

80. Arnowitt, R., Dutta, B., Kamon, T., and Tanaka, M., *Phys. Lett.*, **B538**, 121–129 (2002).
81. Dedes, A., Dreiner, H. K., and Nierste, U., *Phys. Rev. Lett.*, **87**, 251804 (2001).
82. Babu, K. S., and Kolda, C. F., *Phys. Rev. Lett.*, **84**, 228–231 (2000).
83. Mizukoshi, J. K., Tata, X., and Wang, Y., *Phys. Rev.*, **D66**, 115003 (2002).
84. Baer, H., and Balazs, C., *JCAP*, **0305**, 006 (2003).
85. Baer, H., Belyaev, A., Krupovnickas, T., and Mustafayev, A., *JHEP*, **06**, 044 (2004).
86. Baer, H., Balazs, C., Belyaev, A., Krupovnickas, T., and Tata, X., *JHEP*, **06**, 054 (2003).
87. Baer, H., Krupovnickas, T., and Tata, X., *JHEP*, **07**, 020 (2003).
88. Baer, H., Belyaev, A., Krupovnickas, T., and Tata, X., *JHEP*, **02**, 007 (2004).
89. Baer, H., Krupovnickas, T., and Tata, X., *JHEP*, **06**, 061 (2004).
90. Baer, H., Balazs, C., Belyaev, A., and O'Farrill, J., *JCAP*, **0309**, 007 (2003).
91. Abrams, D., et al., *Phys. Rev.*, **D66**, 122003 (2002).
92. Benoit, A., et al., *Phys. Lett.*, **B545**, 43–49 (2002).
93. Spooner, N., *eConf*, **C010630**, P401 (2001).
94. Bernabei, R., et al., Dama results (2003), astro-ph/0305542.
95. Bravin, M., et al., *Astropart. Phys.*, **12**, 107–114 (1999).
96. Akerib, D. S., et al., First results from the cryogenic dark matter search in the soudan underground lab (2004), astro-ph/0405033.
97. Klapdor-Kleingrothaus, H. V., Dietz, A., and Krivosheina, I. V., *Nucl. Phys. Proc. Suppl.*, **124**, 209–213 (2003).
98. Cline, D. B., et al., *Nucl. Phys. Proc. Suppl.*, **124**, 229–232 (2003).
99. Suzuki, Y., Low energy solar neutrino detection by using liquid xenon (2000), hep-ph/0008296.
100. Brunetti, R., et al., Warp liquid argon detector for dark matter survey (2004), astro-ph/0405342.
101. Eigen, G., Gaitskell, R., Kribs, G. D., and Matchev, K. T., *eConf*, **C010630**, P342 (2001).
102. de Boer, W., Herold, M., Sander, C., and Zhukov, V., Indirect evidence for the supersymmetric nature of dark matter from the combined data on galactic positrons, antiprotons and gamma rays (2003), hep-ph/0309029.
103. Hooper, D., and Wang, L.-T., *Phys. Rev.*, **D69**, 035001 (2004).
104. Jungman, G., Kamionkowski, M., and Griest, K., *Phys. Rept.*, **267**, 195–373 (1996).
105. Feng, J. L., Matchev, K. T., and Wilczek, F., *Phys. Lett.*, **B482**, 388–399 (2000).
106. Feng, J. L., Matchev, K. T., and Wilczek, F., *Phys. Rev.*, **D63**, 045024 (2001).
107. Baer, H., and O'Farrill, J., *JCAP*, **0404**, 005 (2004).
108. Carmona, E., *Nucl. Phys. Proc. Suppl.*, **95**, 161–164 (2001).
109. Ahrens, J., et al., *Nucl. Phys. Proc. Suppl.*, **118**, 388–395 (2003).
110. Halzen, F., and Hooper, D., *JCAP*, **0401**, 002 (2004).
111. Mayer-Hasselwander, H. A., et al., High-energy gamma ray emission from the galactic center (1998), mPE-440.
112. Morselli, A., Lionetto, A., Cesarini, A., Fucito, F., and Ullio, P., *Nucl. Phys. Proc. Suppl.*, **113**, 213–220 (2002).
113. Elsaesser, D., and Mannheim, K., Supersymmetric dark matter and the extragalactic gamma ray background (2004), astro-ph/0405235.
114. de Boer, W., Herold, M., Sander, C., and Zhukov, V., *Eur. Phys. J.*, **C33**, s981–s983 (2004).
115. de Boer, W., et al., Excess of egret galactic gamma ray data interpreted as dark matter annihilation (2004), astro-ph/0408272.
116. Pearce, M., *Nucl. Phys. Proc. Suppl.*, **113**, 314–321 (2002).
117. Casaus, J., *Nucl. Phys. Proc. Suppl.*, **114**, 259–273 (2003).
118. DuVernois, M. A., et al., *Astrophys. J.*, **559**, 296–303 (2001).
119. Baltz, E. A., Edsjo, J., Freese, K., and Gondolo, P., *Phys. Rev.*, **D65**, 063511 (2002).
120. Orito, S., et al., *Phys. Rev. Lett.*, **84**, 1078–1081 (2000).
121. Matchev, K. T., and Pierce, D. M., *Phys. Lett.*, **B467**, 225–231 (1999).
122. Baer, H., Drees, M., Paige, F., Quintana, P., and Tata, X., *Phys. Rev.*, **D61**, 095007 (2000).
123. Barger, V. D., and Kao, C., *Phys. Rev.*, **D60**, 115015 (1999).
124. Hinchliffe, I., Paige, F. E., Shapiro, M. D., Soderqvist, J., and Yao, W., *Phys. Rev.*, **D55**, 5520–5540 (1997).
125. Georgi, H., Quinn, H. R., and Weinberg, S., *Phys. Rev. Lett.*, **33**, 451–454 (1974).
126. Georgi, H., and Glashow, S. L., *Phys. Rev. Lett.*, **32**, 438–441 (1974).

127. Buras, A. J., Ellis, J. R., Gaillard, M. K., and Nanopoulos, D. V., *Nucl. Phys.*, **B135**, 66–92 (1978).
128. Murayama, H., and Pierce, A., *Phys. Rev.*, **D65**, 055009 (2002).
129. Hebecker, A., and March-Russell, J., *Nucl. Phys.*, **B613**, 3–16 (2001).
130. Hall, L. J., and Nomura, Y., *Phys. Rev.*, **D64**, 055003 (2001).
131. Kobakhidze, A. B., *Phys. Lett.*, **B514**, 131–138 (2001).
132. Altarelli, G., and Feruglio, F., *Phys. Lett.*, **B511**, 257–264 (2001).
133. Kawamoto, T., and Kawamura, Y., Symmetry reduction, gauge transformation and orbifold (2001), hep-ph/0106163.
134. Mohapatra, R. N., Unification and supersymmetry (1999), hep-ph/9911272.
135. Gell-Mann, M., Ramond, P., and Slansky, R., *Rev. Mod. Phys.*, **50**, 721 (1978).
136. Fritzsch, H., and Minkowski, P., *Ann. Phys.*, **93**, 193–266 (1975).
137. Raby, S., *Rept. Prog. Phys.*, **67**, 755–811 (2004).
138. Altarelli, G., and Feruglio, F., Models of neutrino masses and mixings (2004), hep-ph/0405048.
139. Gell-Mann, M., Ramond, P., and Slansky, R., Complex spinors and unified theories (1980), print-80-0576 (CERN).
140. Yanagida, T., Horizontal gauge symmetry and masses of neutrinos (1979), in Proceedings of the Workshop on the Baryon Number of the Universe and Unified Theories, Tsukuba, Japan, 13-14 Feb 1979.
141. Mohapatra, R. N., and Senjanovic, G., *Phys. Rev. Lett.*, **44**, 912 (1980).
142. Fukuda, Y., et al., *Phys. Rev. Lett.*, **82**, 2644–2648 (1999).
143. Fukuda, S., et al., *Phys. Rev. Lett.*, **85**, 3999–4003 (2000).
144. Buchmuller, W., Neutrinos, grand unification and leptogenesis (2002), hep-ph/0204288.
145. Ananthanarayan, B., Lazarides, G., and Shafi, Q., *Phys. Rev.*, **D44**, 1613–1615 (1991).
146. Anderson, G., Raby, S., Dimopoulos, S., Hall, L. J., and Starkman, G. D., *Phys. Rev.*, **D49**, 3660–3690 (1994).
147. Carena, M., Olechowski, M., Pokorski, S., and Wagner, C. E. M., *Nucl. Phys.*, **B426**, 269–300 (1994).
148. Rattazzi, R., and Sarid, U., *Phys. Rev.*, **D53**, 1553–1585 (1996).
149. Ananthanarayan, B., Shafi, Q., and Wang, X. M., *Phys. Rev.*, **D50**, 5980–5984 (1994).
150. Blazek, T., Raby, S., and Tobe, K., *Phys. Rev.*, **D60**, 113001 (1999).
151. Baer, H., Diaz, M. A., Ferrandis, J., and Tata, X., *Phys. Rev.*, **D61**, 111701 (2000).
152. Auto, D., Baer, H., Belyaev, A., and Krupovnickas, T., Reconciling neutralino relic density with yukawa unified supersymmetric models (2004), hep-ph/0407165.
153. Baer, H., and Ferrandis, J., *Phys. Rev. Lett.*, **87**, 211803 (2001).
154. Feng, J. L., Kolda, C. F., and Polonsky, N., *Nucl. Phys.*, **B546**, 3–18 (1999).
155. Bagger, J., Feng, J. L., and Polonsky, N., *Nucl. Phys.*, **B563**, 3–20 (1999).
156. Bagger, J. A., Feng, J. L., Polonsky, N., and Zhang, R.-J., *Phys. Lett.*, **B473**, 264–271 (2000).
157. Baer, H., Mercadante, P., and Tata, X., *Phys. Lett.*, **B475**, 289–294 (2000).
158. Baer, H., et al., *Phys. Rev.*, **D64**, 015002 (2001).
159. Baer, H., Diaz, M. A., Quintana, P., and Tata, X., *JHEP*, **04**, 016 (2000).
160. Auto, D., et al., *JHEP*, **06**, 023 (2003).
161. Blazek, T., Dermisek, R., and Raby, S., *Phys. Rev. Lett.*, **88**, 111804 (2002).
162. Blazek, T., Dermisek, R., and Raby, S., *Phys. Rev.*, **D65**, 115004 (2002).
163. Dermisek, R., Raby, S., Roszkowski, L., and Ruiz De Austri, R., *JHEP*, **04**, 037 (2003).